



## Review

## Vehicle emissions trapping materials: Successes, challenges, and the path forward

Jungkuk Lee<sup>a</sup>, Joseph R. Theis<sup>b</sup>, Eleni A. Kyriakidou<sup>a,\*</sup><sup>a</sup> Department of Chemical and Biological Engineering, University at Buffalo, The State University of New York, Buffalo, NY, 14260, USA<sup>b</sup> Chemical Engineering Department, Ford Motor Company, 2101 Village Road, Dearborn, MI, 48124, USA

## ARTICLE INFO

## Keywords:

Cold-start  
Hydrocarbon traps  
Passive NOx adsorbers  
Traps  
Emissions control

## ABSTRACT

The modern three-way catalyst (TWC) is very effective for treating the hydrocarbons (HCs), carbon monoxide (CO), and nitrogen oxides (NOx) from stoichiometric gasoline engines once the TWC has achieved its minimum operating temperature (e.g., 250 to 400 °C, depending on the gas species). Likewise, the diesel oxidation catalyst (DOC), selective catalytic reduction (SCR) catalyst with urea injection, and the diesel particulate filter (DPF) are effective for treating the HCs, CO, NOx, and particulate matter (PM) emissions from diesel engines once the catalysts are warmed up, although this can require a significant length of time (e.g., 1 to 3 min) because of the relatively low exhaust temperatures from diesel engines. For both types of engines, excess fueling is often used to accelerate the heating of the catalyst system after a cold start, although this decreases the fuel economy of the vehicle. Even with excess fueling, a high portion (up to 80%) of the total vehicle emissions is emitted during the cold start period (i.e., the period before the catalysts are functional). To treat the HC emissions during this cold start period, one approach is to employ a HC trap (HCT) that can adsorb the HC emissions at low temperatures and then oxidize the stored HCs to carbon dioxide (CO<sub>2</sub>) and water (H<sub>2</sub>O) at higher temperatures. To treat the NOx emissions during the cold start period, a passive NOx adsorber (PNA) can adsorb the NOx at low temperatures. For stoichiometric gasoline applications, the PNA can then reduce the stored NOx to nitrogen (N<sub>2</sub>) at higher temperatures. On diesel engines, the PNA can release the stored NOx back into the exhaust once the downstream urea/SCR system is operational. Some adsorber technologies have the capability of adsorbing HCs and NOx simultaneously. In this review, the HC trapping and passive NOx adsorbing technologies will be discussed in separate sections. This review will describe how the current trapping technologies can be applied in vehicle exhaust systems, the material properties required for efficient HCTs and PNAs, and the exhaust conditions that can inhibit/enhance their trapping properties. First, the performance of HCTs will be discussed in terms of their physical properties (e.g., pore size, acidity, presence of metal ions) and the trapping conditions (e.g., storage temperature, space velocity, and the presence of other exhaust species such as H<sub>2</sub>O and CO<sub>2</sub>). This will be followed by in-depth coverage of the reactions occurring during HC desorption. The second part of this review will focus on the composition of various PNA formulations, the effects of the trapping conditions (e.g., temperature, space velocity, the presence of other exhaust species such as CO<sub>2</sub>, H<sub>2</sub>O, CO, and C<sub>2</sub>H<sub>4</sub>), and the effects of sulfur poisoning on their trapping performance. The effect of hydrothermal aging and the regenerability of HCTs and PNAs will also be discussed. A significant amount of literature has emerged recently regarding HCTs and PNAs; this review is primarily focused on summarizing this literature and reconciling the differences presented.

## 1. Introduction

Regulations on vehicle emissions are becoming increasingly stringent around the world due to growing concerns over the impact of air pollution on the environment and public health. These regulations are intended to minimize the emissions of hydrocarbons (HCs), carbon

monoxide (CO), nitrogen oxides (NO + NO<sub>2</sub>, or NOx), and particulate matter (PM) from gasoline and diesel engines [1–3]. Simultaneously, increasingly stringent fuel economy (FE) regulations are being implemented to reduce the emissions of carbon dioxide (CO<sub>2</sub>) from vehicles in an effort to combat global warming [4]. For over 35 years, three-way catalysts (TWCs) have been successfully used on

\* Corresponding author.

E-mail address: [elenikyr@buffalo.edu](mailto:elenikyr@buffalo.edu) (E.A. Kyriakidou).

stoichiometric gasoline engines to convert HCs, CO, and NOx into non-toxic water ( $H_2O$ ),  $CO_2$ , and nitrogen ( $N_2$ ) with high efficiency once the catalyst has achieved its minimum operating temperature after a cold start (e.g., 250 to 400 °C, depending on the exhaust gas species) [5–8]. On diesel engines, the diesel oxidation catalyst (DOC), selective catalytic reduction (SCR) catalyst with urea injection, and diesel particulate filter (DPF) are effective for decreasing the emissions of HCs, CO, NOx, and PM after they have achieved their minimum operating temperatures. However, due to the high mechanical efficiency and lean A/F ratios of the diesel engine, the exhaust temperatures are relatively low [9,10]. Consequently, a significant period of time on the order of 1 to 3 min is required for the diesel emission control system to become effective following a cold start [10–14].

Until the catalyst system reaches its minimum operating temperature after a cold start (i.e., the “cold start period”), most of the emissions from the engine are emitted into the atmosphere [14–17]. Excess fueling is often used to accelerate the warmup of the aftertreatment system on both gasoline and diesel engines. The excess fuel is injected into the combustion chamber late in the combustion process, and the heat from combusting these HCs is used to heat up the catalysts. However, this excess fueling decreases the fuel economy of the vehicle [18]. For gasoline engines, the cold start fueling can also produce additional PM, which can then necessitate the use of a gasoline particulate filter (GPF) to satisfy PM standards [19]. Even with cold start fueling, a high percentage (e.g., 80 to 90%) of the total emissions from the vehicle is emitted during the cold start period [2,3,20]. To achieve the ever-tightening emission standards, the emissions during this period need to be treated.

To address the cold-start problem, several approaches have been considered. One approach involves electrically heated catalysts (EHC), where electric energy from the battery is used to accelerate the warmup of the catalyst. However, the use of EHCs has been rather limited due to high costs and delays in the heat up time [5,21,22]. A more popular approach to reduce the cold start emissions involves the use of close-coupled catalysts, which have been successfully employed on both gasoline and diesel engines to reduce the warmup time [23,24]. For gasoline engines, this required the development of TWCs with improved thermal durability. However, even with close-coupled catalysts, some emissions are still emitted from the vehicle during the period before the catalyst has achieved its operating temperature. In addition, packaging constraints have prevented the implementation of close-coupled catalysts on some applications [21,25].

Another attractive method for treating the HC emissions during the cold start period is to employ a HC trap (HCT). The HCT stores the HC emissions during the cold start period and then converts the stored HCs into  $CO_2$  and  $H_2O$  once the trap has achieved the temperature necessary to oxidize the HCs [26–31] (Fig. 1A). For diesel engines or lean-burn gasoline engines, the excess  $O_2$  can be used to oxidize the stored HCs.

For stoichiometric gasoline engines, a supply of excess  $O_2$  is needed while the stored hydrocarbons are being released. This can be accomplished with air injection or lean engine operation or potentially with materials in the washcoat of the HCT that can provide oxygen during the period while the stored HCs are being released [32]. This will be discussed in more detail in a later section.

To treat the NOx emissions during the cold start period, a passive NOx adsorber (PNA) can be used to store the NOx (Fig. 1B). For stoichiometric gasoline engines, the PNA can then reduce the stored NOx to  $N_2$  using the reductants in the exhaust once the trap has achieved the necessary temperatures. For lean applications such as the diesel engine, the PNA can release the stored NOx back into the exhaust once the downstream SCR catalyst has achieved its minimum operating temperature and the injection of the urea has commenced [6,33,34]. In a 2011 patent by Cavataio et al., HCT and PNA adsorbing materials were combined on the same monolith for the simultaneous remediation of HCs and NOx [35].

HCTs and PNAs have been the focus of significant research because they overcome the limitations of the other leading technologies: e.g., they do not require electrical components, they do not require close-coupled catalysts which can present packaging challenges and/or catalyst durability issues on some applications, and they store much of the emissions that are normally emitted during the cold start period, even on applications with close-coupled converters. In this review, we summarize the results of recent studies on HCTs and PNAs with regard to the properties of the materials used, the trapping conditions, and the hydrothermal stability. First, we will give an overview of the materials used as HCTs and discuss several parameters affecting the trapping properties of zeolite based HCTs (e.g., temperature, HCT volume, pore size, acidity, the presence of metal ions, and the presence of  $H_2O$  and  $CO_2$  in the exhaust). The second part of this review is dedicated to a description of PNA materials, the effects of several parameters affecting the trapping efficiency of PNAs (e.g., temperature, PNA volume, NO concentration, the presence of other exhaust gas species such as  $H_2O$ ,  $CO_2$ , CO, and  $C_2H_4$ ), and their sulfur tolerance. Finally, both the HCT and PNA sections will be followed by a discussion of their regenerability and hydrothermal stability.

## 2. Hydrocarbon traps

Zeolites have become the adsorbing materials of choice for hydrocarbons due to their unique structure and acidic properties [36–39]. These properties allow increased storage capacity at low temperatures and the release of the stored species at high temperatures. Zeolites which are unexchanged are capable of adsorbing long-chain, short-chain, and aromatic HCs such as decane, propene, and toluene, respectively. When the same zeolites were ion-exchanged with certain metal ions, their adsorption efficiency was found to increase. The HC

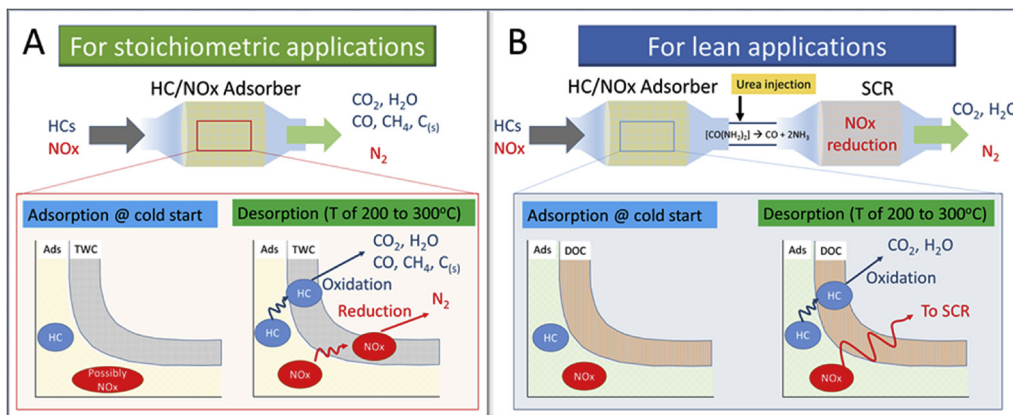


Fig. 1. Configuration of HCTs and PNAs for stoichiometric (A) and lean (B) applications.

adsorption efficiency can be defined as the percentage of the stored HC ( $[HC]_{in} - [HC]_{out}$ ) divided by the feed concentration of the HC during a storage time  $t$ , where  $[HC]_{in}$  and  $[HC]_{out}$  are the HC concentrations in the reactor feed and outlet, respectively (Eq. (1)) [32]:

$$HC \text{ adsorption efficiency} = \left( 1 - \frac{\int_0^t ([HC]_{out}) * \text{flow rate } dt}{\int_0^t ([HC]_{in}) * \text{flow rate } dt} \right) \times 100 \quad (1)$$

The inclusion of the flow rate in Eq. (1) above allows the average HC storage efficiency to be calculated during transient driving conditions, when the flow rate can change rapidly. The HC slip during periods of high flow will influence the average HC adsorption efficiency more than the HC slip during periods of low flow.

The increased HC adsorption efficiency that was observed upon ion-exchanging the zeolites with metal ions was likely due to an increase in the number of adsorption sites [40]. For instance, the ethene ( $C_2H_4$ ) adsorption capacity improved significantly over BEA ion-exchanged with 2.5 wt% silver (Ag) (296  $\mu\text{mol}$ ) compared to unexchanged BEA zeolite (44  $\mu\text{mol}$ ). This may be due to interactions between the  $\pi$ -electrons of the unsaturated HCs and the metal adsorption sites [41]. Increasing the amount of ion-exchanged metal can further increase the number of adsorption sites and consequently the amount of HCs adsorbed. This was indicated by the increase of toluene adsorption with increasing Ag loading over Ag ion-exchanged ZSM-5 zeolites [7,42].

Any catalyst downstream of the HC adsorber will be at a lower temperature than the HC adsorber during a cold start unless some form of external heating is used to preheat those downstream catalysts (e.g., electric heating, gas burners). Consequently, the stored HCs need to be oxidized on the HC trap itself. Therefore, a layer of a TWC catalyst is usually applied on top of the HC adsorber layer to oxidize the hydrocarbons as they are released from the adsorber layer [43–45]. The TWC layer needs to become active for HC oxidation before the stored hydrocarbons are released from the adsorber layer so that the TWC layer can oxidize the hydrocarbons to  $CO_2$  and  $H_2O$  and not merely release the hydrocarbons back into the exhaust. In a modeling study, Goralski et al. showed that the optimal ratio of the adsorber and oxidation catalyst layers for minimizing the total HC (THC) emissions on a vehicle during Bag 1 of the Federal Test Procedure (FTP) was at a loading of 65% adsorber and 35% TWC [46].

The volume of the HCT influences the time required for the TWC layer to become catalytically active. Yamamoto et al. showed that increasing the volume of the HC trap (and therefore the amounts of the adsorber layer and the oxidation layer) slowed down its heating rate, which decreased the HC desorption rate but also delayed the activation (or “light-off”) of the TWC layer (Fig. 2). As a result, the conversion of the adsorbed HCs was not improved [47].

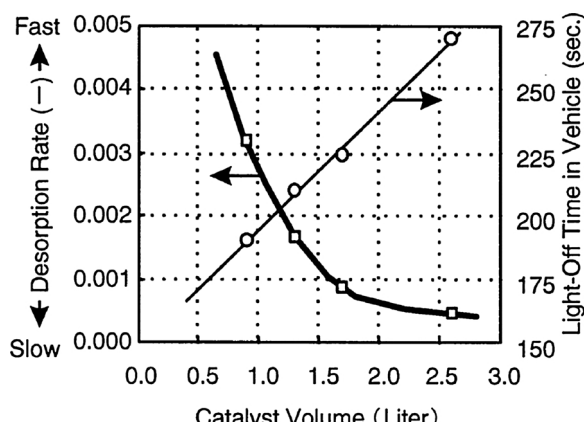


Fig. 2. Desorption rate and light-off time as a function of the HCT volume. Reprinted from Yamamoto et al. [47], Copyright© (2000), with permission from SAE International.

The oxidation of the released HCs requires a source of excess  $O_2$ . For diesel or lean-burn gasoline applications, there is always plenty of excess  $O_2$  available for oxidizing the hydrocarbons. However, a significant challenge for stoichiometric gasoline engines is the lack of sufficient  $O_2$  for the HC oxidation while they are being released. One method to accomplish this is to run the engine lean during the period that the HCs are being released. However, this would result in high levels of NOx slip during this time since the entire catalyst system would be exposed to lean conditions. Another method is to run the engine at stoichiometry but use an air pump to inject air into the exhaust downstream of the close-coupled TWC so that the TWC can continue to reduce NOx while the hydrocarbons are being oxidized on the HC trap. However, in addition to the added cost of the air pump and associated control system, air injection upstream of the HCT prevents any unreduced NOx from the close-coupled TWC from being reduced on the HCT [48,49]. In theory, oxygen storage capacity (OSC) materials such as ceria could be included in the TWC layer to provide the oxygen for the oxidation reactions [50–52]. However, current OSC materials typically do not become active for oxygen storage and release until ca. 300 to 350 °C, which is significantly above the range of temperature where the stored hydrocarbons are released (e.g., 200–250 °C). This approach would become more feasible if OSC materials are developed that can provide oxygen storage and release at lower temperatures (e.g., 200 °C).

## 2.1. Properties of hydrocarbon adsorbing materials

### 2.1.1. Pore size and volume of zeolites

Small pore zeolites are more durable compared to large pore zeolites, and for that reason their use for automotive applications is preferred [53]. In addition, large pore zeolites (e.g., BEA) in SCR catalysts can store a large amount of HCs at low temperatures, such as during extended idles. If the exhaust temperature increases rapidly to high temperatures for a DPF regeneration or a desulfation, the oxidation of the stored HCs can destroy the zeolite [53,54]. Small pore chabazite zeolites are able to prevent the storage of large HCs at low temperatures [53], although Pd on chabazite has been observed to store ethene (unpublished data by J. Theis).

For HCT applications, the pore size of zeolites can affect their HC adsorption capacity. Small pore zeolites cannot store large HC molecules, such as toluene, because the large molecules cannot penetrate the small pore openings. For example, Ca5 A zeolites, which have a relatively small pore size (5.0  $\times$  5.0 Å), displayed much lower adsorption efficiency (4%) for propene, toluene, and decane than larger pore HY (44%), H $\beta$  (36%), HMOR (56%), and HZSM-5 (62%) zeolites [23]. Similarly, SSZ-33 zeolite displayed higher toluene adsorption capacity (1.8 mmol/g) than MCM-68 (1.2 mmol/g) due to its larger ring size (i.e., 12-membered ring vs. 10-membered ring) [55]. Furthermore, Park et al. demonstrated an increase in toluene adsorption capacity with increasing zeolite ring and channel size: USY > X, Beta > M10, and ZSM-5 > FER [56].

Another issue with small pore zeolites is that large molecules can block the pore mouths. In addition, small molecules, e.g. alkenes, under certain conditions can undergo oligomerization reactions, forming larger molecules that can also block the pore-mouth of small pore zeolites (see Section 2.3) [57]. Isobutene, for instance, can react with the zeolite acid sites to produce oligomers that can block the zeolite pores. The effect of oligomerization can be more prominent in small pore zeolites [24].

Therefore, because of their increased HC adsorption capacity and the ability to store larger HC molecules, larger pores tend to help. However, large pore zeolites are less hydrothermally stable compared to small pore zeolites [53]. Moreover, small HCs cannot be efficiently adsorbed by large pore zeolites. A potential solution to this problem is to polymerize the small HCs (< 4 carbon atoms) to larger HCs (5–8 carbon atoms) by using a polymerization catalyst upstream of the HCT [58].

There are practical limits to increasing the ring size of the zeolite. However, it is possible to construct zeolites with both micropores and mesopores. The micro/mesoporous zeolites have a hierarchical structure because the mesopores are a scale above the micropores in size. Such zeolites are alternatively called bimodal because there is a discontinuous increase in size from micro to meso pores. Li et al. demonstrated that bimodal micro/mesoporous MOR zeolites provided more accessible adsorption sites compared to the parent MOR, leading to enhanced toluene – zeolite interactions [59]. Another advantage of the micro/mesoporous structure is that the bimodal MOR displayed a higher toluene desorption temperature (246 °C) compared to the parent (without mesopores) MOR (224 °C). This is desirable for HC trapping applications, as the higher desorption temperature allows more time for the top TWC layer to become active for oxidizing the released HC. In contrast, a separate study reported that bimodal H-ZSM-5 (meso/H-ZSM-5) showed lower propene and toluene adsorption capacity compared to conventional H-ZSM-5 during cold-start tests due to its reduced micropore volume (0.10 and 0.18 cm<sup>3</sup>/g, respectively) [22].

Taken together, the examples above indicate that large pore zeolites are preferred for storing large HCs. However, large pore zeolites are less hydrothermally stable compared to small pore zeolites, and this aspect limits their effectiveness for adsorbing and releasing hydrocarbons over the life of the vehicle. Therefore, the development of large pore zeolites with high hydrothermal stability remains a challenge to date. A potential solution would be the synthesis of hydrothermally stable hierarchical zeolites with tuned mesoporosity.

### 2.1.2. Al content – zeolite acidity

The Si/Al ratio is known to determine the acidic properties of zeolites, and this has a major influence on efficiency of hydrocarbon adsorption and desorption [60]. For example, it was reported that the HC (propene, toluene, decane) adsorption efficiency increased from 18 to 44% when the Si/Al ratio was decreased from 100 to 5 in HY zeolites [23]. The HC adsorption efficiency of zeolites may be understood from the mechanism of HC adsorption. HCs can adsorb on both Lewis and Brönsted acid sites. Hydrogen bonding has been proposed as the mechanism for the adsorption of propene, a representative alkene, on the OH groups of the Brönsted acid sites. Specifically, the π-electrons of the alkene (C=C) are proposed to hydrogen bond with the H of the –OH group [61]. Consistent with this, there is an experimentally observed correlation between the amount of propene adsorbed and the number of Brönsted acid sites. For example, the amount of propene adsorbed over HY zeolite (277 μmol/g) was found to be of similar magnitude to the number of Brönsted acid sites (172 μmol/g) [60]. However, toluene can interact with the Lewis acid sites, the framework oxygen, and potentially the Brönsted acid sites of the zeolites as well [21,62,63]. Low Si/Al ratio HY (2.5) zeolites showed an increased toluene adsorption compared to higher Si/Al ratio HY zeolites (15, 100) in dry conditions [60]. Potential explanations were (1) interaction between the aromatic toluene ring and the Lewis acid sites (electron-deficient sites) and (2) interaction between the negatively charged oxygen of the framework and the toluene methyl group [23,41,60]. Other researchers attributed the origin of toluene adsorption to an electrostatic interaction between the Brönsted acid sites of the zeolite and the delocalized π-system of toluene [21,62,63]. Unlike propene and toluene, the interactions of decane with the zeolite are nonspecific in nature, induced by dispersive forces [41]. Decane, as a saturated and hydrophobic HC, has a higher affinity towards high Si/Al ratio zeolites. These zeolites tend to have a hydrophobic nature, attributed to the low concentration of OH groups of the Brönsted acid sites. For instance, decane showed the highest adsorption capacity over high Si/Al ratio HY (100) zeolite (172 μmol/g), compared to lower Si/Al ratio HY (15) (106 μmol/g) and HY (2.5) (72 μmol/g) zeolites [60].

In addition to maximizing the adsorption of HCs, the release of the HCs should occur at temperatures above the lightoff temperature of the TWC layer. The acidity of the zeolites, which is associated with the Si/

Al ratio, influences the temperature at which the HCs are released. Therefore, when optimizing zeolites for releasing HCs at the desired temperature, the Si/Al ratio is one of the essential parameters to tune. Unsaturated HCs adsorb stronger over low Si/Al ratio zeolites that have high acidity, resulting in high desorption temperatures [59,64]. In one study, the toluene desorption temperature over unexchanged ZSM-5 zeolites increased from 144 to 177 °C by decreasing the Si/Al ratio from 140 to 15 [65]. Lupescu et al. showed that the acidity of the zeolite in HC adsorbers can also be increased by incorporating an acidic oxide (e.g. alumina, silica-alumina, sulfated zirconia) into the beta-zeolites. The improved Brönsted acidity induced by the oxide resulted in an increased adsorption of small HCs (e.g. ethene, propene) and their release at high temperatures [66]. Increasing the Lewis acidity by ion-exchanging the zeolites can also increase the desorption temperature. Specifically, ion-exchanged zeolites of increasing Lewis acidity, H-ZSM-12 < Na-ZSM-12 < Ag/ZSM-12 led to increasing ethene desorption temperatures, 246.7 °C < 277.2 °C < 336.4 °C, and increasing toluene desorption temperatures, 255.2 °C < 287 °C < 357.7 °C, respectively, when the heating rate was 3 °C/s [62].

These studies indicate that the adsorption of unsaturated/saturated HCs depends on the zeolite acidity. While low acidity zeolites favor the adsorption of saturated HCs, high acidity zeolites are preferred for the adsorption of unsaturated HCs. Moreover, high acidity zeolites are able to interact strongly with unsaturated HCs, resulting in higher desorption temperatures that are desired for HC adsorbers. Therefore, for the efficient adsorption of hydrocarbons on a HC adsorber, the acidity of the zeolites should be taken into consideration along with the type(s) of HCs that need to be adsorbed. The HC adsorber should have a combination of low acidity zeolites and high acidity zeolites so it can store the various HCs that are emitted from an engine during the cold start.

### 2.1.3. Presence of metal cations

As discussed in Section 2, ion-exchanged zeolites contain metal cations which replace the original cations. The ion-exchanged metal cations can induce Lewis acidity, resulting in different HC adsorption and desorption properties compared to unexchanged zeolites [40,67,68]. Herein, the effect of different types of metal cations, e.g. alkali metals, silver, copper, and platinum, on the HC adsorption/desorption properties of the zeolites will be discussed.

**2.1.3.1. Alkali metal cations.** The majority of studies on alkali ion-exchanged zeolites focus on their ability to trap toluene because it is a major component in gasoline. Toluene adsorption can be enhanced over alkali ion-exchanged zeolites compared to their unexchanged forms. Specifically, Na ion-exchanged ZSM-5 (Si/Al = 10) and MOR (Si/Al = 6.5) zeolites showed improved toluene adsorption capacity (0.92 and 1.34 μmole·mg<sup>-1</sup>, respectively) compared to the unexchanged form of the studied zeolites (0.69 and 1.07 μmole·mg<sup>-1</sup>, respectively). Moreover, toluene adsorption increased with increasing Na<sup>+</sup> content due to an increase in the toluene adsorption strength [65,69].

A comparison of different alkali ion-exchanged zeolites showed that the Lewis acidity along with the size of the cation can influence the toluene adsorption. For instance, Na ion-exchanged zeolites showed higher toluene adsorption compared to Cs ion-exchanged zeolites. This behavior was attributed to the smaller ionic diameter of Na<sup>+</sup> compared to Cs<sup>+</sup> ions, which occupy a large volume inside the zeolite channels [64]. However, the higher Lewis acidity of Na<sup>+</sup> could also have contributed to the increased toluene adsorption. Apart from the size of the alkali ion and its Lewis acidity, the charge of framework oxygen (Lewis basicity) plays an important role in toluene adsorption, since it can interact with the methyl group of toluene. The adsorption capacity and desorption temperature of toluene depend on a combination of all the above parameters. For instance, while the Lewis acidity of the alkali metal ions decreased in the following order: Li > Na > K > Rb > Cs, their Lewis basicity followed the exact opposite order. Even though Na

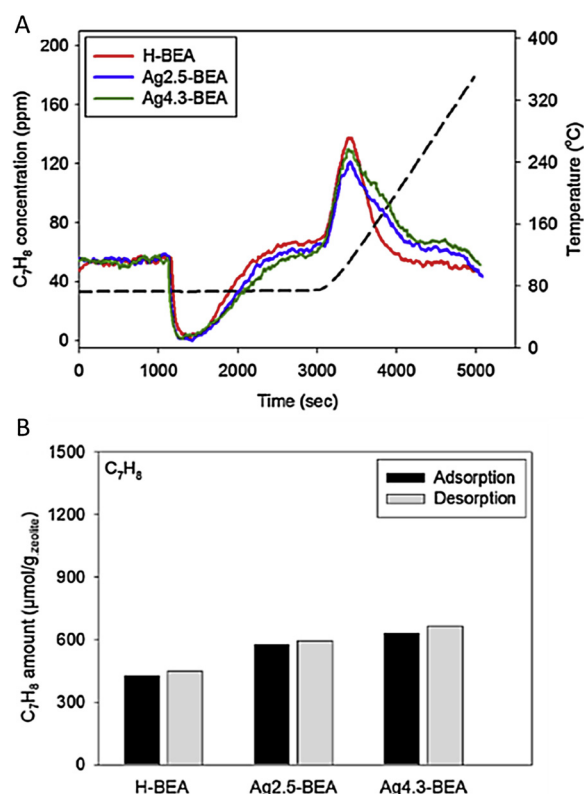


**Fig. 3.** Adsorption/desorption (A) profiles and (B) capacity of toluene as a function of Ag content (Feed: 50 ppm C<sub>7</sub>H<sub>8</sub>, 10% O<sub>2</sub>, 5% H<sub>2</sub>O, N<sub>2</sub> balance, SV: 50,000 h<sup>-1</sup>). An increase of Ag loading in BEA (Si/Al = 19) leads to an increase in the toluene adsorption capacity. Reprinted from Kang et al. [42], Copyright© (2017), with permission from Springer.

has neither the highest Lewis acidity nor basicity, Na ion-exchanged ZSM-5 (Si/Al = 20) and  $\beta$  (Si/Al = 19) zeolites showed a higher toluene desorption temperature compared to the other alkali ions (Na > K, Li > Rb > Cs). These results indicate that Lewis acidity or basicity alone cannot predict the adsorption/desorption properties of the alkali ion-exchanged zeolites, considering that toluene is able to interact with both Lewis acid and base sites [64]. Therefore, the optimal performing zeolite takes into account both Lewis acidity and basicity.

**2.1.3.2. Silver.** Silver ion-exchanged zeolites also showed enhanced toluene adsorption properties compared to zeolites in their unexchanged form [8,42]. For instance, 2.5 wt% Ag ion-exchanged BEA displayed higher toluene adsorption capacity (482 μmol) than an unexchanged BEA zeolites (376 μmol). Moreover, increasing the Ag loading up to 4.3 wt% resulted in even higher toluene adsorption capacity (549 μmol) (Fig. 3). Apart from toluene, Ag ion-exchanged zeolites can also adsorb small HCs (e.g. ethene, propene) [42,70]. The enhanced toluene adsorption over Ag ion-exchanged zeolites is attributed to the strong interaction of the toluene phenyl ring with the Ag ions, since non-ionic Ag showed no adsorption of toluene [71]. Specifically, the intensity of phenyl ring vibrations (1602 and 1495 cm<sup>-1</sup>) decreased over Ag ion-exchanged ZSM-5 zeolite (phenyl-H<sup>+</sup>), while bands at 1592 and 1487 cm<sup>-1</sup> were generated (phenyl-Ag<sup>+</sup>) (Fig. 4). The new bands had lower wavenumbers compared to the phenyl-H<sup>+</sup> vibrations, suggesting stronger interactions of the phenyl ring with Ag<sup>+</sup> compared to H<sup>+</sup>. Another indication of the strength of the phenyl-Ag<sup>+</sup> interactions was obtained by monitoring the FTIR intensity of the phenyl-Ag<sup>+</sup> bands during desorption at different temperatures. The phenyl-Ag<sup>+</sup> bands maintained their intensity during desorption, whereas the intensities of the phenyl-H<sup>+</sup> bands decreased. The significance of the intensity of the bands is the strength

of interaction.

Apart from the toluene adsorption capacity, the toluene desorption temperature was also affected by ion-exchanging BEA zeolites with Ag. The desorption of toluene over unexchanged BEA zeolites had only one low temperature desorption peak ranging from 80 to 180 °C, which is too low for the TWC layer to be active [42]. After ion-exchanging the BEA zeolite with Ag, a second desorption peak appeared at a higher temperature (180–330 °C). This temperature range is more applicable to cold-start applications, and the TWC layer would be more active in this temperature range. The high temperature desorption peak was attributed to Lewis acid sites generated by the Ag species.

Considering the results above, ion-exchanging zeolites with Ag can improve the adsorption of both small (e.g. ethene, propene) and large (e.g. toluene) HCs. However, the adsorption of small HCs over Ag ion-exchanged zeolites require further investigation since there is limited available information in the literature. Moreover, desorbing toluene at temperatures where the TWC layer is active remains a challenge.

**2.1.3.3. Copper.** Copper (Cu) containing zeolites have been studied by several groups and have shown promising HC trapping performance, especially for unsaturated HCs such as propene and toluene [22,72,73]. In the case of Cu ion-exchanged ZSM-5 zeolites, the HC (propene, toluene) adsorption efficiency increased ( $\geq 47.1\%$ ) compared to unexchanged ZSM-5 zeolites (42.2%) [74]. The increased propene and toluene adsorption capacities can be attributed to the exchanged Cu<sup>x+</sup> sites, which act as Lewis acid centers in the zeolite [41]. However, the adsorption capacity of decane (saturated HC) actually decreased over the Cu ion-exchanged Y zeolites relative to the unexchanged zeolite. As mentioned in Section 2.1.2, the adsorption sites for saturated HCs are non-specific, originating from dispersion interactions with the zeolite pore walls.

In principal, the purpose of HC adsorbing materials is to absorb HC molecules at low temperatures and then oxidize them on the TWC layer of the HCT or the adsorbing material itself at higher temperatures [41,72]. It is important to note that the measured amount of desorbed HCs will be less than the amount of adsorbed HCs if oxidation reactions or partial oxidation reactions have occurred. When unexchanged and 3.4 wt% Cu ion-exchanged Y (2.5) zeolites were used for trapping propene, decane and toluene, a portion of the stored HCs was oxidized to CO and CO<sub>2</sub> (Fig. 5) [41]. The HY generated only low levels of CO<sub>2</sub> at temperatures above 335 °C, while the 3.4 wt% Cu/Y generated much higher CO<sub>2</sub> levels starting at 235 °C, with a peak CO<sub>2</sub> generation at 455 °C. This indicates that the Cu significantly improved the ability of the zeolite to oxidize the stored hydrocarbons to CO<sub>2</sub> (and H<sub>2</sub>O). Similar observations have been reported for Cu ion-exchanged ZSM-5 zeolites that showed the release of only CO<sub>2</sub> during desorption [72].

Similar to alkali metal and Ag containing zeolites, Cu containing zeolites showed an enhanced HC adsorption capacity compared to unexchanged zeolites which is attributed to the introduction of new adsorption sites. Moreover, Cu containing zeolites are able to partially oxidize the adsorbed HCs to CO and CO<sub>2</sub>. A key point is that the oxidation or partial oxidation products must be accounted for when comparing the amount of HC adsorbed and the amount of HC released.

**2.1.3.4. Platinum.** Platinum containing Y zeolites prepared via incipient wetness impregnation showed the same pattern towards propene, toluene and decane adsorption compared to Cu ion-exchanged Y zeolites mentioned in Section 2.1.3.3. Specifically, while the decane (saturated HC) adsorption capacity decreased over the 2.3 wt% Pt/Y zeolites, propene and toluene (unsaturated HCs) adsorption capacity increased [41]. The increased propene and toluene adsorption can be explained by the interaction of the Pt metallic species with the  $\pi$ -electrons of the unsaturated HCs. During desorption, Pt containing Y (2.5) zeolites displayed extensive oxidation of adsorbed toluene and decane to CO<sub>2</sub> starting at 120 °C. The temperature for peak CO<sub>2</sub> generation was at 295 °C, which was

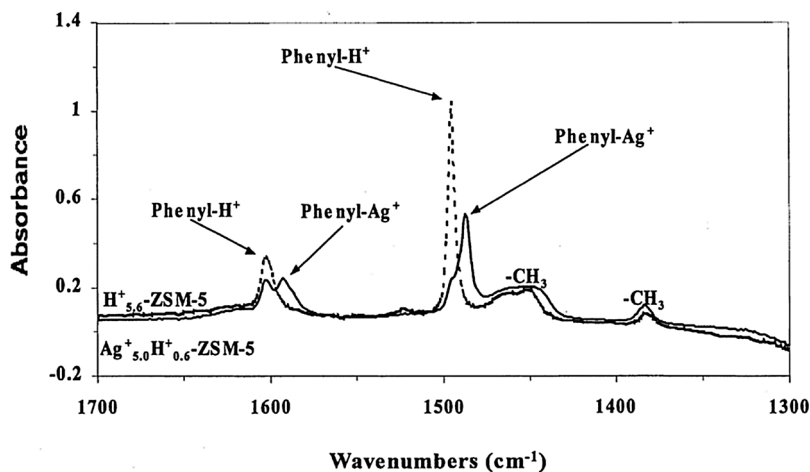


**Fig. 4.** FT-IR spectrum of protonated form ( $\text{H}_5^+ \text{-ZSM-5}$ ) and Ag ion-exchanged ZSM-5 ( $\text{Ag}^+_5 \text{H}^+_{0.6} \text{-ZSM-5}$ ) after toluene adsorption. Ag ion-exchanged ZSM-5 shows new IR bands at lower wavenumbers ( $1592$  and  $1487\text{ cm}^{-1}$ ) compared to protonated form of ZSM-5 zeolite. The new IR band formation is attributed to the strong interaction between phenyl groups and  $\text{Ag}^+$ . Reprinted from Liu et al. [71], Copyright© (2001), with permission from Elsevier.

significantly lower than the peak generation temperatures of  $455\text{ }^\circ\text{C}$  for the copper Y zeolite (Fig. 5) [41]. This behavior was attributed to the presence of reduced Pt particles and/or PtOx clusters in the zeolites which facilitated the HC oxidation.

## 2.2. Effect of trapping conditions

### 2.2.1. Effect of storage temperature

During actual vehicle operation, the exhaust temperatures are constantly changing, resulting in a varying storage temperature for the HCT. Therefore, the effect of different storage temperatures on the HC adsorption has been investigated in the effort to simulate the engine cold-start phase [24,75]. An example of the effect of different storage temperatures is a decrease in toluene adsorption with increasing adsorption temperature ( $100$ ,  $150$ ,  $200\text{ }^\circ\text{C}$ ) [24,65]. This can be attributed to the decreasing stability of the adsorbed HC species with increasing

temperature as the rate of desorption approaches the rate of adsorption. The exothermic nature of toluene adsorption also contributes to the decreasing capacity with increasing temperature. A decrease in toluene adsorption with increasing temperature from  $250$  to  $400\text{ }^\circ\text{C}$  was also observed over Cs ion-exchanged MOR zeolites [76]. These results indicate that toluene adsorption is not favored at high storage temperatures. Unlike toluene, isobutene adsorption increased with increasing storage temperature over HZSM-5 and HY zeolites [24]. For example, a  $4.55\%$  increase in isobutene adsorption capacity was observed with an increase in storage temperature from  $25$  to  $140\text{ }^\circ\text{C}$  (ZSM-5). An explanation for this enhanced isobutene adsorption with increasing temperature was not given. There has not been an extensive study of the temperature-dependent adsorption of all HCs present in vehicle exhaust up to the date of publication of this review.

Therefore, systematic studies on the effect of storage temperature on the adsorption of all HCs present in the vehicle exhaust can create new

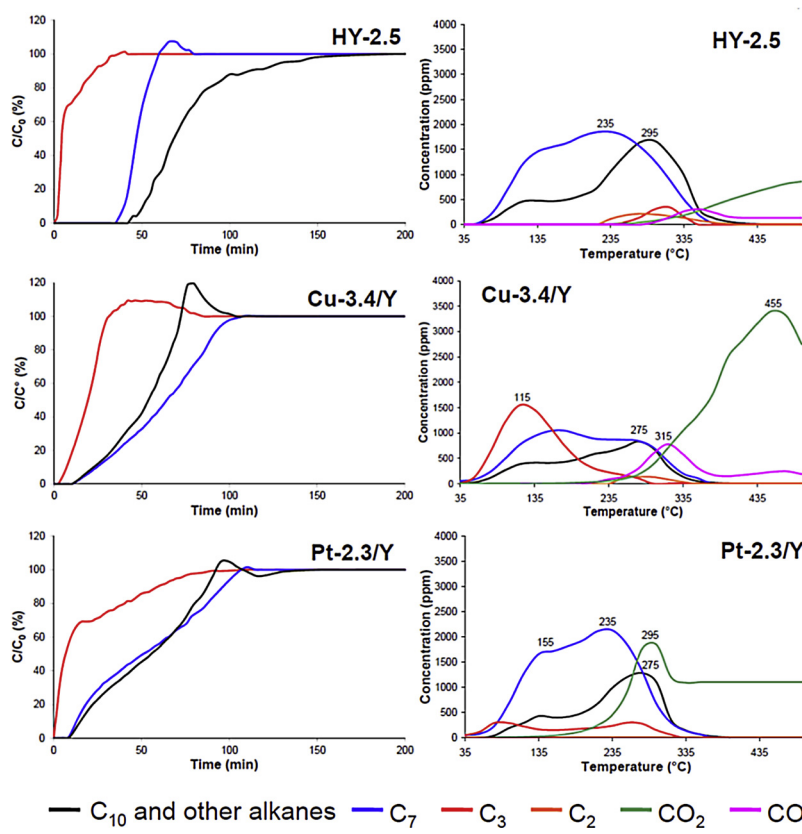


**Fig. 5.** (Left column) breakthrough curves of propene ( $\text{C}_3$ ), toluene ( $\text{C}_7$ ) and decane ( $\text{C}_{10}$ ) mixture and (right column) desorption profiles of pre-adsorbed HC mixture over three different zeolites (HY (2.5), 3.4 wt.% Cu/Y, 2.3 wt.% Pt/Y). Cu and Pt containing zeolites show higher adsorption capacity of unsaturated HCs ( $\text{C}_3$  and  $\text{C}_7$ ), and display higher oxidation ability compared to unexchanged zeolites. Reprinted from Westermann et al. [41], Copyright© (2016), with permission from Elsevier.

research opportunities in the HCT research field.

### 2.2.2. Effect of HCT volume

The volume of the HCT can also play an important role in the reduction of the HC emissions. A larger HCT volume increases the HC storage capacity and simultaneously decreases the warmup rate of the trap that can result in a decrease in the rate of desorption. However, lower warmup rates also delay the lightoff of the TWC layer, which is not desirable for cold start applications (Fig. 2) [47]. A modeling study by Goralski et al. demonstrated that increasing the HCT volume from 500 to 2000 cm<sup>3</sup> on a vehicle reduced the total HC (THC) emissions in Bag 1 of the FTP from around 1.5 g to 1.2 g [46]. However, the decrease in HC emissions diminished as the volume of the HCT continued to increase, as the HC emissions only dropped from 1.2 g to 1.0 g as the volume of the HCT was doubled from 2000 to 4000 cm<sup>3</sup>. These results indicate that both the storage capacity and the warmup rate of the TWC layer of the HCT need to be taken into consideration when optimizing the HCT volume.

### 2.2.3. Effect of HC concentration

The concentration of HCs in the exhaust also influences the adsorption efficiency of the HCT. Because of the limited number of adsorption sites, higher HC concentrations lead to faster saturation of the storage sites. Goralski et al. assessed the trapping performance of a HCT with a mixture of hydrocarbons including ethene, iso-butene, propene, toluene, ethene, and benzene [46]. Following a high temperature purge, the HCT was exposed to total HC concentrations ranging from 500 to 2500 ppm until the trap was saturated. Fig. 6 shows the total moles of HC adsorbed per volume as a function of the HC concentration. Since the trap followed the Langmuir isotherm, the trap stored more HCs as the concentration increased, as shown in Fig. 6A. However, the decreasing slope of the curve in Fig. 6B indicates a decreasing storage efficiency (i.e., increasing HC slip) as the feedgas HC concentration increased (Eq. (1)).

### 2.2.4. Multi-HC adsorption/desorption

Actual vehicle exhaust contains a variety of HCs. In these multi-HC feed streams, each HC species competes for the same adsorption sites and can hinder the diffusion of other HC species through the pores during adsorption and desorption. An example that illustrates this point is the simultaneous adsorption of propene and toluene over ZSM-5 zeolites. Propene molecules diffuse faster than toluene and occupy the zeolite acid sites first, limiting the adsorption of the slower-diffusing toluene molecules [5]. Furthermore, the presence of multiple HCs can also affect the desorption temperature. For instance, bulkier HCs can sterically hinder the diffusion of smaller HCs through the zeolite pores. This concept, known as single-file diffusion, was introduced by Czaplowski et al. and is applicable to 1-dimensional (1-D) channel zeolites

[25]. Based on this concept, the desorption temperature of smaller molecules (e.g. propene) in a multi-HC feed can be increased compared to that of a single-HC feed.

Apart from the HC molecule size and the rate with which they can diffuse, the strength of their interaction with the zeolite adsorption sites plays a pivotal role on their adsorption as well. Several studies demonstrated that the HC that is able to interact stronger with the adsorption sites can displace another initially adsorbed HC [8,77]. For example, adsorption of a ternary HC mixture (propene, toluene, decane) over HY and H $\beta$  zeolites showed competitive adsorption between the toluene and the decane. Toluene, which is able to diffuse faster than decane, arrived at the adsorption sites first [5]. However, decane subsequently arrived and replaced the toluene because decane interacted more strongly with the zeolite pore walls. Similar competitive adsorption was also reported for the following binary HC systems: propene-decane [5], isopentane-toluene [8], and ethene-toluene [42] over unexchanged 5 A, BEA, and ion-exchanged Ag/BEA zeolites, respectively. The degree of competitive adsorption can also be affected by the Si/Al ratio of zeolites. For instance, increasing the Si/Al ratio of HY zeolites from 2.5 to 100 led to displacement of more toluene molecules by decane (Fig. 7) [60]. As mentioned in Section 2.1.2, decane adsorption is favored in high Si/Al ratio zeolites due to their high hydrophobicity.

### 2.2.5. Effect of H<sub>2</sub>O

Vehicle exhaust contains 5–13 % H<sub>2</sub>O that can significantly decrease the HC adsorption capacity of adsorbing materials such as zeolites [56,71]. As a result, the inhibition by H<sub>2</sub>O significantly decreases the HC adsorption efficiency of HC adsorbers in vehicle exhaust systems [78]. Specifically, MeAPO-36, ZSM-22, and ZSM-23 zeolites showed ~ 50% reduction in their ethene and toluene adsorption capacity when H<sub>2</sub>O was introduced into the reactor [79]. This behavior was attributed to the competition of water and HC molecules for the same adsorption sites. On the other hand, the presence of H<sub>2</sub>O can enhance the adsorption of water-soluble compounds, e.g. ethanol, due to their high solubility in water [48]. However, most species in gasoline and diesel exhaust are insoluble in water. As a result, H<sub>2</sub>O inhibition is still a major challenge for HCT technology. One potential way to reduce the water effect is to use high Si/Al ratio zeolites. These zeolites have hydrophobic properties compared to low Si/Al ratio zeolites and thus reduce the water inhibition effect [60]. For instance, the iso-pentane elution time over BEA200 (Si/Al<sub>2</sub> = 200) was longer compared to BEA38 (Si/Al<sub>2</sub> = 38) in the presence of water, indicating that BEA200 was able to adsorb iso-pentane more effectively than BEA38 under these conditions [80]. This is because the HCs interact more strongly with zeolites with higher Si/Al ratios in the presence of H<sub>2</sub>O. Moreover, the calculated heat of adsorption ( $-\Delta H$ ) of iso-pentane in the presence of 5.4% H<sub>2</sub>O was 45.5 and 50.1 kJ/mol over BEA38 (low Si/Al) and BEA200 (high Si/Al), respectively. This means that the adsorption of

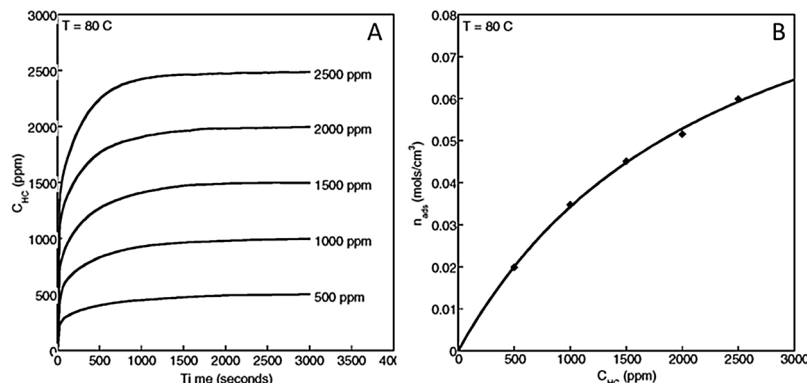


**Fig. 6.** (A) HC adsorption isotherms and (B) total moles of HC adsorbed for different HC concentrations. Reprinted from Goralski et al. [46], Copyright© (2000), with permission from SAE International.

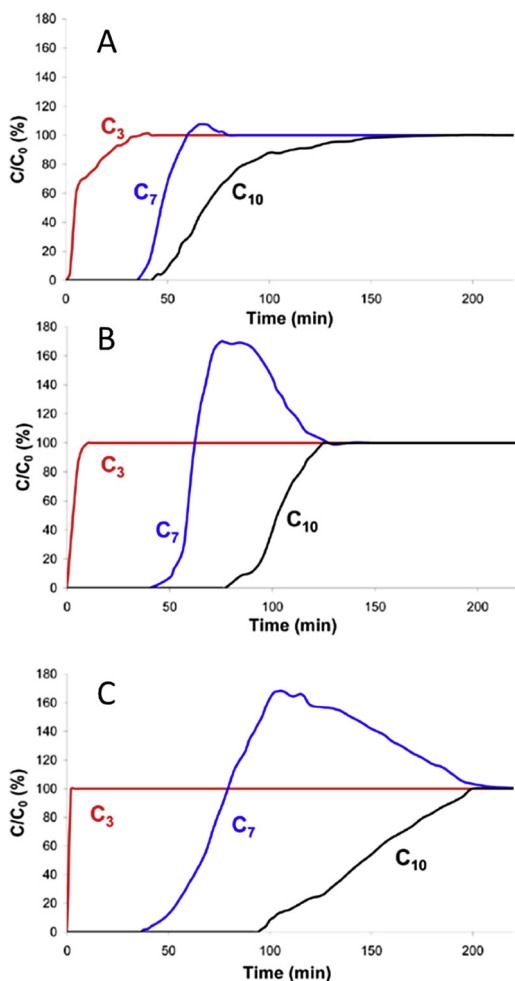


**Fig. 7.** Adsorption breakthrough curves of a HC mixture ( $C_3$  = propene,  $C_7$  = toluene,  $C_{10}$  = decane) over unexchanged HY zeolites with different Si/Al ratios in the absence of water: (A) Si/Al = 12.5, (B) Si/Al = 15, (C) Si/Al = 100. Competitive adsorption between  $C_7$  and  $C_{10}$  is more prominent over higher Si/Al zeolites. Reprinted from Azambre et al. [60], Copyright© (2015), with permission from ACS publications.

iso-pentane over the BEA200 zeolite is a more exothermic process and as a result more enthalpically favorable. However, even though high Si/Al ratio zeolites can reduce the inhibition from water, they have fewer adsorption sites relative to low Si/Al ratio zeolites. As a result, gains made by increasing the Si/Al ratio are minimized or even eliminated. An ideal zeolite would have a large number of adsorption sites as well as resistance to water inhibition.

An alternate path for reducing the water effect while simultaneously maintaining a high HC adsorption capacity is to ion-exchange the zeolites with metal cations [64]. Among a variety of ion-exchanged zeolites, Ag ion-exchanged zeolites showed the greatest resistance to water inhibition. Sarshar et al. demonstrated that Ag/ZSM-12 experienced less water inhibition than H, Na, Mg, and Fe/ZSM-12 for ethene and toluene [21]. This behavior was attributed to the hydrophobic properties of Ag [81]. These properties were confirmed in another study which monitored the toluene adsorption over Ag ion-exchanged ZSM-5 zeolites with FTIR (Fig. 8) [71]. While the phenyl- $H^+$  band ( $1495\text{ cm}^{-1}$ ) disappeared in the presence of water, the intensity of the phenyl- $\text{Ag}^+$  band ( $1487\text{ cm}^{-1}$ ) showed no significant change. These results suggested that water had no major effect on the toluene-Ag $^+$  interaction. Density functional theory (DFT) calculations have been conducted comparing toluene and water adsorption on unexchanged ( $H^+$ ) and Ag $^+$  ion-exchanged ZSM-5 zeolites [7]. These studies

indicated that the heat of adsorption of toluene was stronger on Ag $^+$  than on  $H^+$ . Meanwhile, the heat of adsorption of water was weaker on Ag $^+$  than  $H^+$ . These calculations confirmed that Ag $^+$  is more resistant to water inhibition than  $H^+$ . Finally, apart from tuning the zeolite properties for mitigating the water inhibition effect, different zeolites can be combined in the zeolite layer. For example, studies by Yeon et al. and Adamczyk et al. demonstrated the use of multi-layered zeolites in HCTs, where zeolites A and 4 A served as water adsorbing materials while zeolites beta and ZSM-5 served as HC adsorbers [78,82]. Lafyatis et al. reported that the presence of a H<sub>2</sub>O trap (zeolite 5 A) and a HC adsorber (H-ZSM5 or H-Beta) absorbed the H<sub>2</sub>O and HC and prevented these species from inhibiting the CO conversion of a downstream Pd-Pt oxidation catalyst. With an enriched A/F ratio to provide more CO and air injection to provide a net lean environment, the CO conversion of the oxidation catalyst was significantly improved. The resulting exotherm from CO oxidation heated up the rest of the catalyst and improved the HC conversion of the system [83].

#### 2.2.6. Effect of CO<sub>2</sub>

CO<sub>2</sub> and H<sub>2</sub>O can both inhibit HC adsorption to different degrees, depending on the zeolite. Sarshar et al. showed that the adsorption of toluene and ethene over unexchanged, ion-exchanged Na-ZSM-12, and ferrisilicate analogs of ZSM-12 zeolite (Fe-ZSM-12) were inhibited more by H<sub>2</sub>O than by CO<sub>2</sub> [21]. However, in the case of Ag/ZSM-12, toluene adsorption was inhibited more by CO<sub>2</sub> than by H<sub>2</sub>O. The inhibitory effect of CO<sub>2</sub> is attributed to its interaction with the negatively charged oxygen (basic sites) neighboring the metal cation. Specifically, the strength of this interaction depends on the strength of the basic site, i.e. weaker Lewis acidity of the metal cation corresponds to stronger framework oxygen basicity. For example, Ag ion-exchanged ZSM-12 was less affected by the presence of CO<sub>2</sub> compared to unexchanged and Na ion-exchanged ZSM-12. This is because the relatively strong Lewis acidity of Ag/ZSM-12 induced weak basicity of framework oxygen, which led to weaker CO<sub>2</sub>-base site interactions.

In contrast, CO<sub>2</sub> can mitigate the effect of H<sub>2</sub>O on the HC adsorption capacity of some zeolites, e.g. TAPO-5, FAPO-36, SAPO-36 and SAPO-5 [79]. A plausible explanation for this behavior is that under wet conditions, CO<sub>2</sub> can modify the surface properties of zeolites by reducing the density of polar hydroxyl linkage (T-OH) groups, rendering the zeolite more nonpolar. A nonpolar zeolite is hydrophobic and thus less prone to interact with the polar water molecules.

Despite the research related to the effect of CO<sub>2</sub> on HC adsorption, a consensus among researchers has not yet surfaced.

#### 2.3. Oxidation, oligomerization, cracking and coke formation during HC desorption

For diesel or lean-burn applications, the exhaust contains excess O<sub>2</sub> which facilitates the oxidation of the adsorbed HCs to CO<sub>2</sub> and H<sub>2</sub>O. However, in stoichiometric gasoline applications there is not enough O<sub>2</sub> to fully oxidize all the adsorbed HCs. As a result, some of the adsorbed HCs can be partly oxidized to CO or form CH<sub>4</sub> and coke. Air injection before the HCT is one possible solution to improve the oxidation of the adsorbed HCs. For example, Ballinger et al. demonstrated that air injection reduced the THC emissions from a sport utility vehicle equipped with a close-coupled TWC and an underbody HCT from 0.022 to 0.019 g/mile during Bag 1 of the FTP after the catalysts were rapidly aged to represent high mileage conditions [49]. Similarly, air injection reduced the THC emissions from 0.057 to 0.049 g/mile during FTP tests on an E85 flex fuel vehicle equipped with an aged close-coupled TWC and an underbody HCT designed for use with ethanol fueled vehicles [48].

The oxidation reactions in HCTs likely occur on their oxidation catalyst layer. However, the HC adsorber layer can also act as an oxidation catalyst at elevated temperatures. For example, apart from Cu and Pt containing zeolites that are able to oxidize HCs to CO and CO<sub>2</sub>

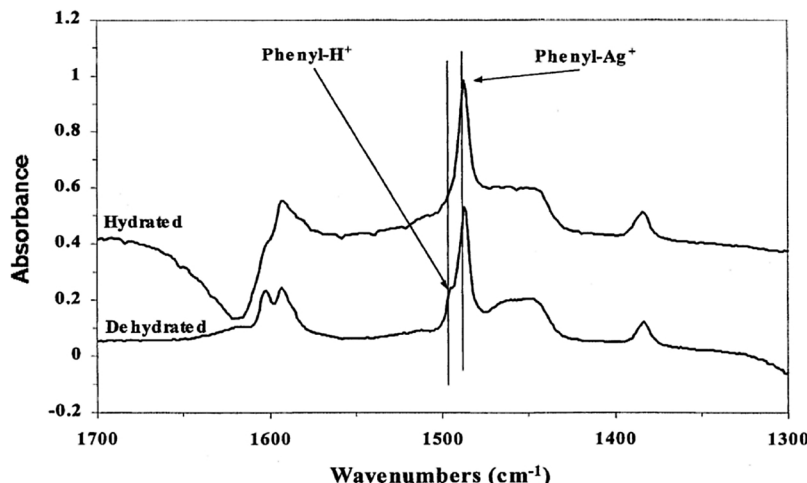


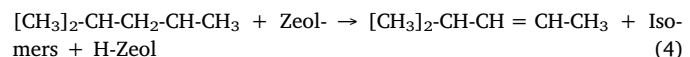
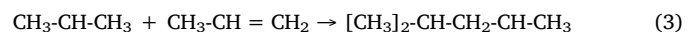
**Fig. 8.** FT-IR spectra of toluene adsorption over hydrated and dehydrated  $\text{Ag}_{5.0}^+\text{H}_{0.6}^+$ -ZSM-5. Reprinted from Liu et al. [71], Copyright© (2001), with permission from Elsevier.

(discussed in Sections 2.1.3.3 and 2.1.3.4), Cs/ZSM-5 showed both a HC adsorption and an oxidation ability [84]. Specifically, a higher percent of oxidized HCs (29%) was observed over Cs/ZSM-5 compared to non-impregnated ZSM-5 zeolites (17%). Part of the adsorbed HC molecules can undergo acid-catalyzed reactions due to the presence of Brønsted acid sites in zeolite adsorbers ( $\text{Al}^--\text{OH}^+-\text{Si}$ ) during the desorption step. This was experimentally observed by the darkening of the samples which denoted coke formation, one of the products of the acid-catalyzed reactions. Coking or transformation of HCs to primary or secondary products prevents an accurate quantification of the adsorbed amounts of each HC during temperature programmed desorption [85,86]. Westermann et al. showed that only a minor fraction (< 25%) of adsorbed propene was recovered during desorption due to these acid-catalyzed reactions over unexchanged  $\text{H}\beta$  (12.5), HMOR (10), and HZSM5 (5.5) zeolites [5]. The generation of ethene and coke (measured by TGA) during desorption confirmed the occurrence of such reactions. Other researchers observed that during desorption, propene converted into ethene, isopentane, and 2-methyl-propene over unexchanged BEA zeolites [8]. Moreover, Aspromonte et al. suggested that toluene decomposition during desorption over Ag ion-exchanged NaMOR zeolites produced primarily coke and hydrogen ( $\text{C}_7\text{H}_8 \rightarrow 7\text{C}(\text{s}) + 4\text{H}_2(\text{g})$ ) [87]. The ability of zeolites to oxidize HCs depends on their Brønsted acidity, with the most acidic zeolite being most active. For instance, the onset temperature of  $\text{CO}_2$  formation decreased from 350 to 340 to 300 °C as the zeolite Brønsted acidity increased with decreasing Si/Al ratio of the HY zeolite from 100 to 15 to 5 [23]. Therefore, a researcher studying high Brønsted acidity zeolites should be especially aware of oxidation reactions that can occur.

Ion-exchanging of zeolites can decrease the amount of carbon formed, i.e. coking, by decreasing the number of Brønsted acid sites in the material [41,88]. Oxidation and coking formation reactions follow the same trend; that is, decreasing the Brønsted acidity decreases the extent of reaction. For instance, Serra et al. showed that the amount of carbon formed over unexchanged HMOR and ion-exchanged  $\text{Cs}_{14}\text{HMOR}$  decreased from 0.039 to 0.028 mg carbon/mg of zeolite [65]. Similarly, Puértolas et al. showed that ion-exchanging H-ZSM-5 and mesoH-ZSM-5 zeolites with Cu completely inhibited the propene oligomerization that was observed over unexchanged H-ZSM-5 and mesoH-ZSM-5 zeolites [22,89]. These studies are consistent with the mechanism of coke formation catalyzed by Brønsted acid sites.

Furthermore, light alkenes are known to be produced during TPD. Work has been conducted to elucidate the mechanisms. One such mechanism is monomolecular cracking [90,91]. One instance of monomolecular cracking is the desorption of ethene from adsorbed toluene over HY (100) zeolites [60]. The alkenes produced by monomolecular

cracking may further react via oligomerization reactions. Oligomerization reactions and subsequent coke formation can occur by interaction of  $\text{C}=\text{C}$  bonds with the OH groups of the zeolite (Eqs. (2)–(4)) [24,60,85]:



Brønsted acid sites in zeolites are also known to donate protons to adsorbed alcohols, leading to their dehydration, e.g. dehydration of ethanol to alkenes that can further oligomerize to higher molecular weight HCs via a carbenium ion mechanism. Nunal et al. showed that adsorbed ethanol can be desorbed as ethene [32]. Subsequently, protonation of ethene by Brønsted acid sites leads to the formation of primary carbenium ions  $\text{ZO}^-\dots\text{CH}_2\text{CH}_3$  that via oligomerization reactions produce 1-butene, 2-butene, and isohexene [92,93]. In contrast to ethene, the protonation of propene leads to the much more stable secondary carbenium ion  $\text{ZO}^-\dots\text{CH}_3^+\text{CH-CH}_3$  that can readily react with adsorbed ethene or propene to give an even more stable tertiary carbenium ion, such as:  $\text{CH}_3\text{-CH}_2^+\text{C}(\text{CH}_3)\text{-CH}_3$ . Desorption of the protonated tertiary carbenium ion leads to 2-methyl butane or isohexene depending on the reactants. These mechanistic studies laid the groundwork for future designs of zeolites with controlled reactivity.

#### 2.4. Regenerability of HC adsorbing materials

In practical applications, the exhaust system undergoes thousands of cold-start cycles during the life of the vehicle [33,94]. The ability of HCTs to maintain their performance through these multiple cycles is an important characteristic. Therefore, it is important to evaluate the performance of HC adsorbing materials during multiple adsorption/desorption cycles to simulate real vehicle operating conditions.

The primary factor for consistent HC trapping performance involves the final temperatures during the previous drive-cycle. If the temperatures are sufficiently high, the adsorber will be thoroughly purged and able to store the maximum amount of HC on the next cold-start. However, if the temperatures at the end of the previous drive-cycle are low (e.g., 100 to 200 °C) for a significant period of time, the adsorber can trap some HCs before the vehicle is shut off. These stored HCs will result in a loss of HC storage capacity during the next cold-start. For gasoline applications, the temperatures are usually sufficiently high to avoid this issue. For diesel engines, however, the temperatures can be

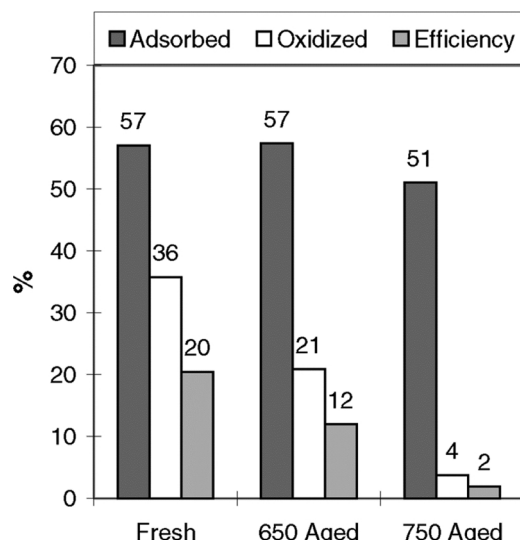


**Fig. 9.** Comparison of adsorption, oxidation, and overall HCT efficiency after Ford 4-mode aging at 650 and 750 °C for 50 h. Reprinted from Goralski et al. [46], Copyright© (2000), with permission from SAE International.

below 200 °C during low load operation, such as during idles or low speed driving conditions. This could result in the adsorption of HC on the adsorber before the vehicle is shut off, leading to reduced trapping performance during the next cold start.

The metal loading of ion-exchanged zeolites is another important parameter for maintaining the performance of the adsorbing materials during cycling. Zeolites with higher metal loading deactivate more. For instance, even though 0.17 wt% Cu/ZSM-5 zeolite was able to adsorb propene and toluene completely for three consecutive cycles, a higher Cu loading (1.12 wt%) displayed deactivation during cycling [72]. This deactivation can be explained by the formation of CuO nanoparticles that could block the access of HCs to the inner pores of the zeolite. Coke formation during desorption can also block the storage sites and result in the partial loss of trapping performance during cycling. However, ion-exchanged Cu/ZSM-5 sample had a lower density of acid sites compared to H-ZSM-5, resulting in slightly lower coke formation. Specifically, the coke formation observed from a TGA analysis over H-ZSM-5 and Cu/ZSM-5 samples was around 4.5 and 3.0 wt%, respectively.

As discussed above, three main aspects have to be considered when investigating the regenerability of HC adsorbers. One of these aspects concerns the exhaust temperatures which need to be high enough, especially for diesel applications, for the HCs to be fully released before the next cycle. Another aspect is the nanoparticle agglomeration during cycling that can block the storage sites. Finally, coke formation should be also taken into account during cycling, especially in cases where there is insufficient oxygen to fully oxidize the HCs.

## 2.5. Durability of HC traps

For real-world applications, automotive HCTs need to be durable to high temperatures. The exhaust exiting the manifold on gasoline engines can reach temperatures as high as 950 °C under high load conditions [95,96]. HC adsorbing materials can undergo structural changes during exposure to such elevated temperatures [97,98]. In the case of zeolites, distortion of the bridging hydroxyl groups at elevated temperatures can be responsible for the zeolite structure collapsing. Severe distortion of bridging hydroxyls ( $Mg-OH-P$ ) in MAPO-5 lattice can lead to the formation of  $Mg-OH$  and  $P-OH$  species at elevated temperatures (700, 800 °C/10 h) [79,99]. Distortion of the bridging hydroxyl groups in zeolites can also result in changes in the zeolite's Brønsted acidity [100,101]. In a separate study of hydrothermally aged

$Ag_{5.0}^{+}H_{0.6}^{+}$ -ZSM-5, Si–OH increased and acidic hydroxyls Si-OH-Al decreased, indicating a reduction in Brønsted acidity [71].

There are a few examples in literature for zeolites used as HC adsorbers that demonstrate good hydrothermal stability, e.g., SSZ-33 (20), ZSM-12 (150), SAPO-5 (0.03) and FAPO-36 (0.05). These zeolites showed no significant structural changes after aging at ~800 °C for 5–10 h compared to their fresh states [40,79,102,103]. This hydrothermal stability was attributed to their stable Si-O-Al and Fe-O-Al bonds [104,105].

Collapsing of the zeolite crystalline structure can lead to a decrease of its HC adsorption capacity [80,106]. For example, after thermal aging of a MCM-68 zeolite (800 °C/5 h), the amount of toluene adsorbed decreased drastically [55]. The reduction of the HC adsorption capacity after thermal aging can be tuned by varying the zeolite Si/Al ratio. Specifically, the HC adsorption capacity of HCTs containing zeolites with low and high Si/Al ratio (40, 180) were similar before thermal aging. However, after aging at 900 °C for 40 h, the amount of HC emissions increased significantly from ~0.39 to 0.85 g/km for zeolites with low Si/Al (40), whereas lower HC emissions (0.51 g/km) were observed for zeolites with high Si/Al (180) [43]. These results indicate that thermal aging has a smaller effect on high Si/Al ratio zeolites even though the HC adsorption capacity of both low and high Si/Al ratio zeolites decreases after aging. However, in a separate study on ion-exchanged La-BEA (10, 300) zeolites, toluene adsorption increased after hydrothermal aging (800 °C/200 h). This behavior was attributed to the adsorption of toluene by extra-framework aluminum sites, which can function as Lewis acid sites. Indeed, using  $^{27}Al$  NMR, tetrahedral (framework) aluminum in fresh La-BEA (10) zeolites was found to migrate to extra-framework positions [86]. Nonetheless, propane adsorption capacity, which occurs on Brønsted acid sites, decreased by more than 75% after the aging.

As discussed in Section 2, HCTs consist of an absorbing and a TWC layer. For a durable HCT, both layers have to maintain their performance after hydrothermal aging. It has been reported by Ford that the overall HCT performance decreased after aging at 650 and 750 °C for 50 h, even though the adsorbing material maintained its adsorption capacity. The decreased HCT performance was therefore attributed to the decreased oxidation performance of the TWC layer after aging (Fig. 9) [46].

The results above indicate that high exhaust temperatures can lead to a collapse of the zeolite structure that results in a decrease in HC adsorption capacity. The reduction of HC adsorption capacity upon hydrothermal aging can be minimized by utilizing high Si/Al ratio zeolites. Deactivation of the oxidation catalyst of the HCT can also occur after hydrothermal aging, resulting in reduction of the total HCT performance. In order to minimize the thermal degradation of the HCT and maintain its trapping capability as well as its ability to oxidize the HCs as they desorb, the HCT can be placed downstream of a close-coupled TWC in a position far from the exhaust manifold. This would reduce the aging temperatures and thereby minimize the thermal degradation of the HCT.

## 3. Passive NO<sub>x</sub> adsorber (PNAs)

While zeolite based materials have been studied broadly for over 25 years as potential HC adsorbers, research into their application as passive NO<sub>x</sub> adsorbers are in a relatively early stage of development. This is largely because oxide based catalysts (e.g., alumina, ceria) were investigated initially for their NO<sub>x</sub> trapping capability. Both classes of catalysts will be discussed in this review. The properties of oxide based materials for NO<sub>x</sub> adsorption/desorption will be discussed first. This will be followed by a discussion of zeolite based materials for passive NO<sub>x</sub> adsorption/desorption.

### 3.1. Properties of PNA materials

#### 3.1.1. Metal oxides for passive NO<sub>x</sub> adsorption

Precious metals, such as Pt and Pd, supported on oxide supports (e.g. CeO<sub>2</sub>, Al<sub>2</sub>O<sub>3</sub>, CeO<sub>2</sub>/ZrO<sub>2</sub>) have been studied extensively for NO<sub>x</sub> trapping applications [12,107,108]. Similar to the HC trapping efficiency defined earlier, the average NO<sub>x</sub> storage efficiency (NSE) is defined as the percentage of the stored NO<sub>x</sub> ([NO<sub>x</sub>]<sub>in</sub> – [NO<sub>x</sub>]<sub>out</sub>) divided by the feed concentration of NO<sub>x</sub> integrated over a storage time t, where [NO<sub>x</sub>]<sub>in</sub> and [NO<sub>x</sub>]<sub>out</sub> are the NO<sub>x</sub> concentrations in the reactor feed and outlet, respectively (Eq. (5)) [12]:

$$\text{NSE} = \left( 1 - \frac{\int_0^t ([\text{NO}_x]_{\text{out}}) * \text{flow rate } dt}{\int_0^t ([\text{NO}_x]_{\text{in}}) * \text{flow rate } dt} \right) \times 100 \quad (5)$$

The inclusion of the flow rate in Eq. (5) above allows the average NO<sub>x</sub> storage efficiency to be calculated during transient driving conditions, when the flow rate can change rapidly.

The presence of precious metals can significantly improve the NSE of the oxide supports. Jones et al. demonstrated that CeO<sub>2</sub> with deposited Pt or Pd nanoparticles showed higher NSE compared to pure CeO<sub>2</sub> [12]. Between Pt and Pd, Pt/CeO<sub>2</sub> showed higher NSE compared to Pd/CeO<sub>2</sub> at 120 and 160 °C (Fig. 10). This can be explained by the formation of different NO<sub>x</sub> adsorption species with these metals [13,33,108]. Specifically, a NO-DRIFTS study over Pt containing catalysts showed strong bands assigned to bridging and monodentate nitrate species and weak bands assigned to mono- and bi-dentate nitrites [12]. This suggested that the Pt oxidized the NO to NO<sub>2</sub> and stored the NO<sub>2</sub> as nitrates at temperatures of 120 °C and above. In contrast, Pd/CeO<sub>2</sub> displayed a strong nitrite band but a weak nitrate band. Nitrate species are more thermally stable than nitrite species, which can account for the higher NSE of Pt/CeO<sub>2</sub>. However, the formation of nitrates can decrease its NO<sub>x</sub> desorption efficiency (NDE), since nitrate species are more difficult to decompose than nitrites. Specifically, nitrite species decomposed and released NO at low temperatures (< 350 °C), while the nitrate species decomposed and released NO<sub>2</sub> at temperatures significantly above 350 °C. Since the temperatures of diesel exhaust are often below 350 °C during low to moderate load operation, the high desorption temperature of nitrates can present difficulties in regenerating the catalyst and preparing it for the next cold start [11,33]. Therefore, although Pt/CeO<sub>2</sub> showed higher NSE, Pd/CeO<sub>2</sub> is more desirable for NO<sub>x</sub> adsorption applications because it can store more NO<sub>x</sub> as nitrite species and thereby release the stored NO<sub>x</sub> more easily during normal driving conditions. This can result in more consistent NO<sub>x</sub> storage performance during successive cold-starts.

Theis et al. compared the NO<sub>x</sub> storage and release performance of monolithic catalysts containing either 0.43 g/L Pt or Pd on washcoats of

ceria/zirconia (CZO) or Al<sub>2</sub>O<sub>3</sub> [107]. On transient tests performed on a reactor partially simulating the exhaust temperatures of a diesel engine during Bags 1 and 2 of the light-duty Federal Test Procedure (FTP) followed by a US06 test, H<sub>2</sub>O suppressed the storage of NO on all four catalysts at temperatures below 100 °C, attributable to condensed H<sub>2</sub>O blocking the storage sites. Above 100 °C, the oxidized Pd/CZO catalyst stored much more NO<sub>x</sub> than the oxidized Pd/Al<sub>2</sub>O<sub>3</sub> catalyst, suggesting that the ceria is very important in the NO<sub>x</sub> storage process when the catalyst is oxidized. However, after rich reductions, both the Pd/CZO and Pd/Al<sub>2</sub>O<sub>3</sub> catalysts stored significantly higher amounts of NO<sub>x</sub>, suggesting that reduced Pd is effective for storing NO<sub>x</sub>. Fig. 11 shows the cumulative amount of NO<sub>x</sub> stored on Pt/Al<sub>2</sub>O<sub>3</sub>, Pt/CZO, Pd/Al<sub>2</sub>O<sub>3</sub>, and Pd/CZO catalysts over the entire Bag 1 + Bag 2 + US06 simulations. Ideally, the cumulative NO<sub>x</sub> would return to zero at the end of the transient test, indicating that all of the stored NO<sub>x</sub> had been released. The oxidized Pd/CZO catalyst released the stored NO<sub>x</sub> much more completely than the oxidized Pd/Al<sub>2</sub>O<sub>3</sub> or Pt/CZO catalysts during the tests, attributed to the Pd/CZO storing more NO<sub>x</sub> as nitrates instead of nitrates.

Crocker et al. investigated Pt and Pd on pure ZrO<sub>2</sub> washcoats for NO<sub>x</sub> adsorption (M. Crocker, personal communication, August 2014). However, this work was terminated due to difficulties with desorbing the stored NO<sub>x</sub> from the Pt/ZrO<sub>2</sub> and Pd/ZrO<sub>2</sub> catalysts. For both catalysts, DRIFTS work indicated that very little NO<sub>x</sub> was desorbed even after exposure to 500 °C.

A potential way to enhance the NO<sub>x</sub> storage/release capability of oxide based trapping materials is by doping them with other metals. For instance, Ji et al. reported that the NSE of 1 wt% La-promoted Pt/Al<sub>2</sub>O<sub>3</sub> was twice as high as that of undoped Pt/Al<sub>2</sub>O<sub>3</sub> for short storage times (< 5 min.), attributable to an increase in the number of NO<sub>x</sub> adsorption sites [108]. However, while the addition of La improved NO<sub>x</sub> adsorption, it was not beneficial for NO<sub>x</sub> desorption because La<sub>2</sub>O<sub>3</sub> largely stored the NO<sub>x</sub> as nitrate species.

Improving the number of oxygen vacancies in the support can decrease the formation of nitrates and enhance the formation of nitrite species, which improves the regenerability of the PNA. As mentioned earlier, Pt oxidizes NO to NO<sub>2</sub> and preferentially stores NO<sub>x</sub> as nitrates, which are difficult to decompose. Addition of Pr to Pt/CeO<sub>2</sub> led to the generation of more nitrite species, attributed to the formation of oxygen vacancies created by Pr-doping in the CeO<sub>2</sub> lattice as shown in Eqs. (6) and (7) [33].



Apart from Pt and Pd oxide based PNAs, Ag/Al<sub>2</sub>O<sub>3</sub> was also reported to be a potential PNA material [95]. The NO<sub>x</sub> storage capacity of Ag/

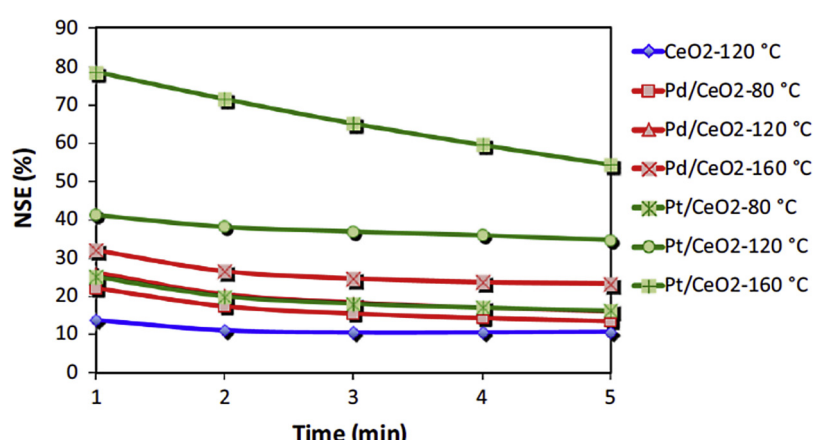


**Fig. 10.** NO<sub>x</sub> storage efficiency of CeO<sub>2</sub> at 120 °C and Pt/CeO<sub>2</sub>, Pd/CeO<sub>2</sub> at 80, 120, and 160 °C. Conditions: 300 ppm NO, 5% O<sub>2</sub>, 5% CO<sub>2</sub>, 3.5% H<sub>2</sub>O, balance He. Reprinted from Jones et al. [12], Copyright© (2016), with permission from Springer.

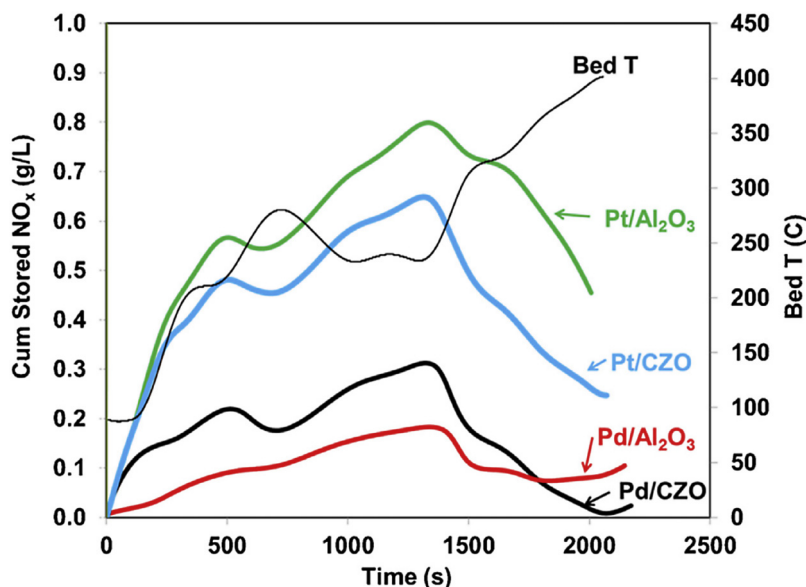


**Fig. 11.** Cumulative amount of NO<sub>x</sub> stored on Pt/Al<sub>2</sub>O<sub>3</sub>, Pt/CZO, Pd/Al<sub>2</sub>O<sub>3</sub>, and Pd/CZO during transient tests performed on a reactor. Reprinted from Theis. [107], Copyright© (2016), with permission from Elsevier.

Al<sub>2</sub>O<sub>3</sub> increased from 0.19 to 0.24 g/L with increasing Ag loading from 0.7 to 3.4 wt%. However, the majority of NO<sub>x</sub> was adsorbed as nitrates and NO<sub>x</sub> desorption was observed at temperatures as high as 430 °C. Therefore, poor regenerability of Ag/Al<sub>2</sub>O<sub>3</sub> PNAs can inhibit the use of these materials in particle applications and it has to be further investigated.

### 3.1.2. Zeolites for passive NO<sub>x</sub> adsorption

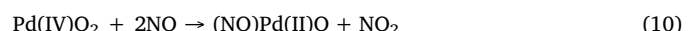
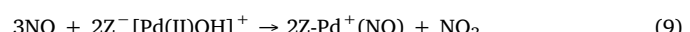
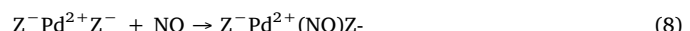
Research on zeolite based PNAs has intensified in recent years. Calcium oxide (CaO) and palladium (Pd) containing zeolites were both investigated as passive NO<sub>x</sub> adsorption materials [75,109]. The addition of 5 wt% CaO to BEA zeolites increased the NO<sub>x</sub> storage capacity and thereby increased the time before NO<sub>x</sub> slip was observed. The NO<sub>x</sub> slip time was further increased by increasing the CaO loading from 5 to 10 wt%. However, increasing the CaO loading to 15 wt% inhibited the NO<sub>x</sub> adsorption, attributed to the excess CaO decreasing the available pore volume of the zeolite. NO<sub>x</sub> molecules were adsorbed on the CaO surface as nitrate species (NO<sub>3</sub><sup>-</sup>) [109], which as mentioned earlier can lead to issues with the regenerability of the PNA.

Significant research into Pd containing zeolites [e.g., BETA (BEA), ZSM-5 (MFI), chabazite (CHA), and OFF, LTL framework zeolites] for NO<sub>x</sub> storage has emerged recently [75,110,111]. Zeolite-based PNAs offer significant advantages over the oxide-based PNAs in regards to tolerance to H<sub>2</sub>O at low temperatures. The zeolite-based PNAs also offer much higher tolerance to sulfur poisoning relative to oxide-based PNAs. These properties will be discussed in more detail later.

It was demonstrated that the NO<sub>x</sub> adsorption capacity and the desorption temperature were influenced by the framework structure of the zeolite [75]. For instance, the NO storage capacities of Pd-CHA, Pd-MFI, and Pd-BEA at 100 °C were 48, 58 and 64 μmol/g, while the temperatures for peak NO<sub>x</sub> release were 360, 275, and 260 °C, respectively. This was attributed to the zeolites having different effects on the electronic properties of the Pd that generate unique NO<sub>x</sub> storage and release characteristics for the different Pd/zeolite combinations.

Ion-exchanging palladium with zeolites can result in the formation of multiple Pd species. Zheng et al. reported that palladium can replace either one (Z<sup>-</sup>H<sup>+</sup>[Pd(OH)]<sup>+</sup>Z<sup>-</sup>) or two (Z<sup>-</sup>Pd<sup>2+</sup>Z<sup>-</sup>) protons in the zeolite framework to form ionic Pd that is dispersed within SSZ-13 (similar framework as CHA with high silica content), BEA, and ZSM-5 zeolites, while some of the palladium generates PdO and PdO<sub>2</sub> on the external surfaces of the zeolites [6]. The distribution of Pd species was

influenced by the zeolite pore size. Specifically, 0.5 wt% Pd/BEA (large pore) and 0.48 wt% Pd/ZSM-5 (medium pore) zeolites had similar amounts (~75%) of ionic Pd atomically dispersed at the cationic sites of the zeolites (as measured by NaCl titration), whereas 0.5 wt% Pd/SSZ-13 (small pore) had only 1.4% ionic Pd. This behavior was attributed to the small pore size of SSZ-13 preventing Pd from penetrating the pore mouths, resulting in the formation of PdOx on the external surface of the zeolites. Similarly, Ryou et al. showed that different Pd/SSZ-13 synthesis methods, e.g. ion-exchange (ION), incipient wetness impregnation (IWI), wet impregnation (WI), and solid-state ion exchange (S-S), resulted in the formation of mostly PdO in SSZ-13 zeolites [34]. However, PdO can be re-distributed to ionic Pd after hydrothermal aging at 750 °C for 25 h. In terms of NO<sub>x</sub> storage, both ionic Pd and PdOx were able to adsorb NO<sub>x</sub> under dry conditions (Eqs. (8)–(10)) [6]:



Pd(IV) was reduced to Pd(II) by NO, and the Pd(II) further acted as a NO<sub>x</sub> adsorption site. Specifically, XPS data showed that pre-oxidized Pd/SSZ-13 contained 75.6% Pd(IV) and 24.4% Pd(II). After reaction with NO, Pd(IV) decreased to 13.9%, whereas Pd(II) increased to 86.1%, indicating the reduction of Pd(IV) to Pd(II) by NO. However, in the presence of water, the NO<sub>x</sub> adsorption efficiency at 120 °C was substantially decreased from 1.08 to 0.14 NO<sub>x</sub>/Pd over 0.88 wt% Pd/SSZ-13 (which contained 90.9% PdOx), indicating that the NO<sub>x</sub> adsorption of PdOx was inhibited in the presence of H<sub>2</sub>O [6]. The re-distribution of PdO to ionic Pd observed after hydrothermal aging led to an increase in NO<sub>x</sub> storage capacity over Pd/SSZ-13 zeolites, indicating that ionic Pd is the active site in the presence of H<sub>2</sub>O [34].

Pd and CaO containing zeolites have both been studied as potential PNAs. However, Pd/zeolite PNAs have attracted significantly more attention. The NO<sub>x</sub> adsorption site on Pd/zeolite PNAs differs depending on whether water is present or not. Both ionic Pd and PdOx are able to adsorb NO<sub>x</sub> in dry conditions, whereas only ionic Pd can adsorb NO<sub>x</sub> in wet conditions at low temperature (< 100 °C). Since water is always present in the vehicle exhaust, the formation of ionic Pd in zeolites is desirable to ensure enhanced NO<sub>x</sub> adsorption.

### 3.2. Effect of trapping conditions

#### 3.2.1. Effect of storage temperature

The amount of NOx adsorption can be increased by increasing the storage temperature. For instance, Jones et al. reported that the NSE increased over both Pt/CeO<sub>2</sub> and Pd/CeO<sub>2</sub> with an increase in storage temperature [12]. This was attributed to an increase in the mobility of oxygen on the CeO<sub>2</sub> surface that can lead to higher NOx adsorption capacity. In addition, Pt/CeO<sub>2</sub> displayed higher NSE than Pd/CeO<sub>2</sub> at different storage temperatures (80, 120, 160 °C). This is because Pt/CeO<sub>2</sub> is more active than Pd/CeO<sub>2</sub> for oxidizing NO to NO<sub>2</sub>, and the rate of this reaction increases as the storage temperature increases. The resulting NO<sub>2</sub> can then be adsorbed in the form of nitrates on Pt/CeO<sub>2</sub>, resulting in the higher NSE. However, the Pd/CeO<sub>2</sub> was easier to regenerate and released a higher portion of the stored NOx below 300 °C, while the Pt/CeO<sub>2</sub> released much of the stored NOx above 300 °C. This is because the Pd/CeO<sub>2</sub> stored much of the NOx as nitrites, while the Pt/CeO<sub>2</sub> stored more of the NOx as nitrates. For both catalysts, the overall NDE after ramping to 500 °C decreased with increasing storage temperature due to the increasing stability of the adsorbed NOx species. A similar increase in NSE with increasing storage temperature was noted over Pt/Al<sub>2</sub>O<sub>3</sub> and La doped Pt/Al<sub>2</sub>O<sub>3</sub> [108]. Specifically, the NSE of Pt/Al<sub>2</sub>O<sub>3</sub> increased from 30% to 60% during the first minute of adsorption with an increase in the adsorption temperature from 80 to 160 °C. However, the NDE below 250 °C decreased with increasing storage temperature due to the increasing formation of nitrates.

Regarding the Pd/zeolites, Chen et al. showed that the NOx storage capacity of the Pd-BEA catalyst decreased with increasing temperature between 80 and 150 °C, while the NOx storage capacity of the Pd-CHA catalyst increased with increasing temperature between 80 and 170 °C. The NOx storage capacity of the Pd-MFI catalyst passed through a maximum between 80 and 170 °C [75,112]. These differences in temperature dependence were attributed to differences in the NO binding strength.

Collectively, these studies indicate that there is a tradeoff between an increase in NSE and a decrease in NDE observed over oxide based PNAs with increasing storage temperature. On the other hand, the effect of storage temperature on zeolite based PNAs does not follow a specific pattern and depends heavily on the zeolite structure. However, our knowledge on the effect of the storage temperature on NOx adsorption/desorption over zeolite based PNAs is currently limited, and further in-depth studies will be advantageous.

#### 3.2.2. Effect of space velocity

Space velocity is a measure of the exhaust flow rate relative to the catalyst volume. An increase in space velocity (SV), either by increasing the flow rate or by decreasing the volume of the catalyst, can lead to a decrease in NSE, because the NOx storage sites become saturated more quickly. Theis et al. reported that with an increase in space velocity from 7.5 K h<sup>-1</sup> to 30 K h<sup>-1</sup>, the NOx slip time over Pd/CZO decreased from 340 to 10 s [11]. The effect of decreased NOx slip time due to high SV was also observed over Ag/Al<sub>2</sub>O<sub>3</sub>. Specifically, by increasing the SV, the NSE decreased from 56% (40 K h<sup>-1</sup>) to 34% (80 K h<sup>-1</sup>) over 1.3 wt % Ag/Al<sub>2</sub>O<sub>3</sub>. Also, over 3.4 wt% Ag/Al<sub>2</sub>O<sub>3</sub> the NSE decreased from 57% (40 K h<sup>-1</sup>) to 33% (100 h<sup>-1</sup>) [95].

#### 3.2.3. Effect of NO concentration

Similar to the effect of a higher space velocity, a higher NO concentration will lead to faster saturation of the NOx storage sites. As a result, NOx slip will occur more rapidly. Theis et al. tested three different NO concentration (e.g. 130, 200, 400 ppm) over a monolithic PNA with a Pd/CZO washcoat [11]. The storage efficiency decreased with increasing NO level, as the peak storage efficiencies for the three concentrations were 100, 70, and 54%, respectively. However, the maximum amount of stored NOx was similar for the three NO concentrations, suggesting that the NOx storage efficiency was limited by

the storage capacity of the sample.

#### 3.2.4. Effect of NO vs. NO<sub>2</sub>

PNAs can store NO<sub>2</sub> much more efficiently than NO. Theis et al. showed that a monolithic PNA with a Pd/CZO washcoat stored NO<sub>2</sub> with nearly 100% efficiency during the first 450 s of a transient test [11], even though the bed temperature was below 100 °C for over 2 min and the feedgas contained 5% H<sub>2</sub>O. In contrast, the storage of NO on the Pd/CZO catalyst was completely inhibited by H<sub>2</sub>O at temperatures below 100 °C, and above 100 °C the peak storage efficiency was only 83%. However, the storage of NO<sub>2</sub> led to the formation of nitrates. As a result, the sample was not completely purged by the end of the test, where the maximum temperature was ca. 400 °C. The data suggested that ca. 30% of the stored NOx was retained on the sample at the end of the test. When NO was used in the feedgas instead of NO<sub>2</sub>, most of the stored NOx was released from the sample by the end of the test, attributable to the formation of nitrites which are easier to decompose. To the best of our knowledge, there are no publications to date discussing the adsorption of NO<sub>2</sub> over zeolite based PNAs.

#### 3.2.5. Effect of other gases on passive NOx trapping

**3.2.5.1. Effect of H<sub>2</sub>O on oxide based PNAs.** Similar to HC adsorption, NO<sub>x</sub> adsorption is also inhibited in the presence of water. Literature studies showed that H<sub>2</sub>O and NOx can compete for adsorption sites, leading to a reduction in NOx adsorption capacity [108,113]. Theis et al. showed that the NOx storage efficiency was substantially suppressed in the presence of water for monolithic PNA samples containing either Pd or Pt on washcoats of CZO or Al<sub>2</sub>O<sub>3</sub> when the catalyst bed temperature was < 100 °C. The decreased NOx storage at temperatures < 100 °C was attributed to water condensation on the storage sites that can hinder the adsorption of NOx [11,13].

Jones et al. studied the combined effect of H<sub>2</sub>O and CO<sub>2</sub> on the PNA performance [21]. The results indicated an inhibitory effect on NSE when both H<sub>2</sub>O and CO<sub>2</sub> were present. For instance, the NSE of Pt or Pd over CeO<sub>2</sub> was reduced by almost 50% in the presence of H<sub>2</sub>O and CO<sub>2</sub> [12,33]. However, the absence of H<sub>2</sub>O and CO<sub>2</sub> promoted the formation of nitrates on both Pt/CeO<sub>2</sub> and Pd/CeO<sub>2</sub>. In contrast, the presence of H<sub>2</sub>O and CO<sub>2</sub> promoted the formation of nitrites on the Pt/CeO<sub>2</sub> or Pd/CeO<sub>2</sub> surface, which is desirable for trapping applications [12].

**3.2.5.2. Effect of H<sub>2</sub>O on zeolite based PNAs.** Similar to the water inhibition effects on the NOx adsorption and desorption of oxide based PNAs discussed in Section 3.2.5.1., the NOx adsorption/desorption over zeolite based PNA materials is also impeded by the presence of water but to a lesser extent. Specifically, CaO containing beta zeolites showed a decrease in NO penetration time (time required for NO to be detected in the reactor outlet) from 38 to 20 min with increasing water concentration from 0.6 to 7.29% in the feed gas [109]. This was attributed to water molecules partially occupying the NO adsorption sites (e.g. CaO). Specifically, water molecules are able to interact with CaO to form Ca(OH)<sub>2</sub> during adsorption at 40 °C that can subsequently react with NO<sub>x</sub> to form Ca(NO<sub>3</sub>)<sub>2</sub>, and this Ca(NO<sub>3</sub>)<sub>2</sub> sterically hinders NOx adsorption. In addition, for adsorption temperatures lower than 100 °C, HNO<sub>2</sub> and/or HNO<sub>3</sub> can be formed via reaction of H<sub>2</sub>O with NO<sub>x</sub>, and this can also reduce the adsorption capacity of CaO-beta samples.

The water inhibition effect is significantly less for Pd containing zeolites. Chen et al. explored the effect of water on the NO adsorption of Pd/chabazite at 100 °C [75]. In a NO-DRIFTS study under dry conditions, it was observed that Pd/chabazite showed three distinguished FTIR bands at 2151, 1806 and 1863 cm<sup>-1</sup> (Fig. 12). The band at 2151 cm<sup>-1</sup> was assigned to NO<sup>+</sup> adsorption on the Brønsted acid sites, whereas both 1806 and 1863 cm<sup>-1</sup> were attributed to linear nitrosyl species on the Pd<sup>2+</sup> ions. In wet conditions, however, only the band at 2151 cm<sup>-1</sup> disappeared, indicating that water molecules can displace NO<sup>+</sup> stored on Brønsted acid sites but not the NOx stored on the Pd

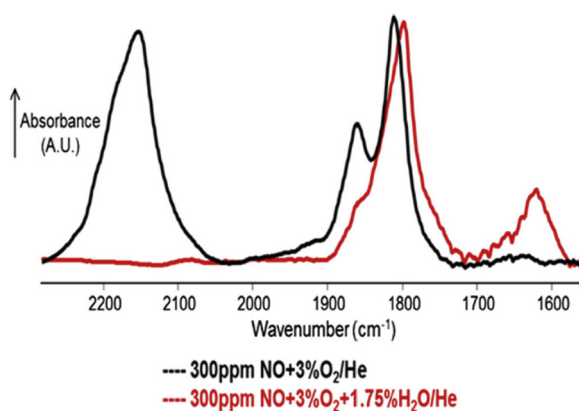


**Fig. 12.** NO-DRIFTS spectra recorded of Pd/chabazite after exposure to 300 ppm NO and 3% O<sub>2</sub> with or without 1.75% H<sub>2</sub>O at 100 °C. Reprinted from Chen et al. [75], Copyright© (2016), with permission from Springer.

sites. Although the band at 1806 and 1863 cm<sup>-1</sup> merged into one single peak at 1798 cm<sup>-1</sup>, its intensity was maintained, suggesting that Pd ions at the exchange sites of the zeolite are able to adsorb NO molecules at low temperatures even in the presence of water. Similar results obtained by Zheng et al. showed that the increasing content of cationic Pd in SSZ-13, BEA and ZSM-5 zeolites can suppress the H<sub>2</sub>O inhibition effect on the NSE [6]. Specifically, the reduction in NSE observed in the presence of H<sub>2</sub>O over Pd/SSZ-13 (87%) < Pd/BEA (78%) < Pd/ZSM-5 (43%) is inversely proportional to the amount of cationic Pd species in the zeolites (9.1, 11.2, 65.3%, respectively). However, ion-exchanging Pd does not completely eliminate water inhibition because a portion of the NO<sub>x</sub> adsorbs on Brønsted acid sites. Moreover, a recent study by Khivantsev et al. attributed the decrease in NO<sub>x</sub> storage capacity in the presence of H<sub>2</sub>O to the formation of stable complexes between H<sub>2</sub>O and Pd (e.g. Pd(H<sub>2</sub>O)<sub>2</sub>(O-Z)<sub>2</sub> or [Pd(OH)<sub>4</sub>]<sup>2-</sup>/[Pd(OH)<sub>3</sub>(H<sub>2</sub>O)]<sup>-</sup>) [114].

The examples discussed in Sections 3.2.5.1 and 3.2.5.2 indicate that both oxide and zeolite based PNAs suffer from water inhibition. Therefore, the hydrophobicity of materials should be taken into account when developing future PNAs.

**3.2.5.3. Effect of CO<sub>2</sub> on zeolite based PNAs.** It has been reported that CO<sub>2</sub> degrades the NO<sub>x</sub> storage efficiency of lean NO<sub>x</sub> traps by competing with the NO<sub>x</sub> for the storage sites (e.g., barium) [115]. Since LNTs and PNAs both function by storing NO<sub>x</sub>, an investigation into the effect of CO<sub>2</sub> on the NO<sub>x</sub> storage and release performance of Pd/zeolite PNAs was warranted. Pihl et al. investigated the effect of CO<sub>2</sub> concentration on the NO<sub>x</sub> storage and release performance of a model Pd/ZSM-5 catalyst [116]. There was essentially no effect on either the NO<sub>x</sub> storage efficiency or the NO<sub>x</sub> desorption efficiency when the CO<sub>2</sub> level was varied from 0 to 13%. This may be explained by the fact that the Pd sites in the PNA can store NO<sub>x</sub> by forming nitrosyls, but they do not store CO<sub>2</sub>. Thus, the CO<sub>2</sub> provides no competition for the NO<sub>x</sub> storage sites in a Pd/zeolite PNA.

**3.2.5.4. Effect of ethene on NO<sub>x</sub> storage.** Under actual vehicle exhaust conditions, NO<sub>x</sub> adsorption can be influenced by the presence of HCs in the exhaust stream. In this regard, the effect of ethene on NO<sub>x</sub> storage over Pd and Pt containing oxide materials has been recently reported [11,107,108]. Theis et al. demonstrated that the presence of ethene can improve the NO<sub>x</sub> storage efficiency of Pd containing ceria/zirconia oxide (Pd/CZO) materials under both dry and wet conditions [107]. Specifically, in the absence of H<sub>2</sub>O, the average NSE while the bed temperature was below 200 °C during transient tests increased from 32% without C<sub>2</sub>H<sub>4</sub> to 49% with C<sub>2</sub>H<sub>4</sub>. A possible explanation of this NSE enhancement is the formation of alkyl nitrites or alkyl nitrates via the interaction between NO and C<sub>2</sub>H<sub>4</sub> [11,108]. However, the formation of these alkyl species could not be confirmed with DRIFTS

analysis due to interference from other species (i.e., carbonates). Contrasting results were obtained for the NSE of Pt/CZO and Pt/Al<sub>2</sub>O<sub>3</sub> from in the presence of C<sub>2</sub>H<sub>4</sub>. Specifically, in the absence of H<sub>2</sub>O, the average NSE while the bed temperature was below 200 °C decreased from 72 to 37% and from 80 to 49% from the addition of C<sub>2</sub>H<sub>4</sub> to the feedgas over Pt/CZO and Pt/Al<sub>2</sub>O<sub>3</sub>, respectively [107]. This decreased NO<sub>x</sub> storage performance was attributed to the C<sub>2</sub>H<sub>4</sub> reducing the NO<sub>2</sub> formed over the Pt back into NO, which is stored less effectively than NO<sub>2</sub>.

The investigation of the effect of hydrocarbons on NO<sub>x</sub> adsorption is still at an elementary stage, and the current reports are non-conclusive. Based on our existing knowledge, it can be concluded that the effect of ethene on NSE over oxide based PNAs depends on the noble metal used. Oxide based PNAs containing Pd showed an increase in NO<sub>x</sub> adsorption capacity in the presence of C<sub>2</sub>H<sub>4</sub>, whereas a decrease in NO<sub>x</sub> storage performance was observed over oxide based PNAs containing Pt. However, since HCs and NO<sub>x</sub> coexist in the vehicle exhaust, understanding of their competitive adsorption will facilitate the use of PNAs in practical applications.

**3.2.5.5. Effect of CO on NO<sub>x</sub> storage.** As mentioned in Sections 3.5.2.1 and 3.5.2.2, water can inhibit NO<sub>x</sub> adsorption. However, the presence of CO in the vehicle exhaust stream can mitigate the water effect either by reducing the Pd to form new adsorption sites or by forming nitrogen-carbon-oxygen (NCO) species on the catalyst surface [6,11,113,117]. For instance, Pd/CZO displayed nearly 100% storage of NO during the first 60 s of adsorption when CO was introduced during transient tests, even in the presence of 5% H<sub>2</sub>O [11]. This behavior was attributed to the formation of NCO species identified during DRIFTS analysis, as indicated in Fig. 13.

Enhancement of NO<sub>x</sub> adsorption in the presence of CO was also observed in the case of Pd containing zeolites. Specifically, under wet conditions (5% H<sub>2</sub>O), the NO<sub>x</sub> adsorption capacity of 1 wt% Pd/BEA increased from 14 to 20 μmol<sub>NOx</sub>/g<sub>cat</sub> in the presence of 225 ppm CO [117]. It was suggested that the enhanced NO<sub>x</sub> adsorption capacity of Pd/BEA in the presence of CO was attributed to the formation of new adsorption sites (reduced Pd) in Pd/BEA. More recently, the increase in NO<sub>x</sub> adsorption capacity of 1 wt% Pd/H-SSZ-13 in the presence of CO was attributed to the formation of the Pd(II)(NO)(CO) complex [114]. Addition of CO in the feed led to a decrease in the 1865 cm<sup>-1</sup> FTIR band, which is assigned to Pd(II)-NO, whereas the band at 1800 cm<sup>-1</sup> increased, which was attributed to the Pd(II)(NO)(CO) complex. It is also possible that the NO and CO interacted to form NCO, similar to the

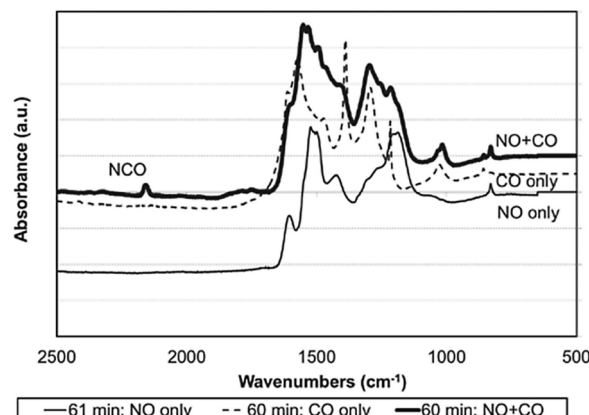


**Fig. 13.** Spectra of diffuse reflectance Fourier transform spectroscopy (DRIFTS) over 2% Pd/ceria (solid line: 300 ppm NO + 5% O<sub>2</sub>, dashed line: 850 ppm CO + 5% O<sub>2</sub>, thick solid line: 300 ppm NO + 850 ppm CO + 5% O<sub>2</sub>). NO<sub>x</sub> adsorption is enhanced in the presence of both CO and NO by formation of NCO species. Reprinted from Theis et al. [11], Copyright© (2017), with permission from SAE International.

case with Pd/CZO. It is conceivable that the mechanism for the enhancement by CO is different for the exchanged (ionic) Pd sites and the unexchanged Pd sites. More research is necessary to identify the mechanism by which CO improves the NO<sub>x</sub> storage efficiency of Pd/zeolite NO<sub>x</sub> adsorbers.

The effect of CO on the NO<sub>x</sub> desorption temperature depends on the type of adsorbing material (zeolite vs. oxide). Specifically, low temperature desorption peaks (100 and 180 °C) were observed in the absence of CO over Pd/BEA [117], which is not desirable for PNA applications. However, in the presence of CO, desorption peaks were observed at higher temperature (160, 260, and 430 °C). The increased NO<sub>x</sub> desorption temperature in the presence of CO was attributed to strong interactions between NO<sub>x</sub> and reduced Pd by CO. In contrast, in the case of MnO<sub>2</sub>/ZrO<sub>2</sub>, the presence of CO led to a decrease of the NO<sub>x</sub> desorption temperature. A study showed a shift in the NO<sub>x</sub> desorption peak from 350 to 210 °C over MnO<sub>2</sub>/ZrO<sub>2</sub> in the presence of CO and H<sub>2</sub>O [113]. This shift of the desorption temperature to a lower temperature region is beneficial for regenerating NO<sub>x</sub> adsorbing materials (see Section 3.4) but can also result in the premature release of some of the stored NO<sub>x</sub> (i.e., before the downstream urea/SCR system is functional). Indeed, when a Pd/CZO catalyst was evaluated for NO<sub>x</sub> storage with CO, some of the stored NO<sub>x</sub> was released at temperatures near 160 °C. This early release was attributed to the instability of NCO [11].

### 3.3. Sulfur poisoning of PNAs

Burning of sulfur containing fuels and the lubricant oils used in vehicles inevitably results in low levels of sulfur oxides (e.g., SO<sub>2</sub>) in the vehicle exhaust. Sulfur oxides are known to cause strong deactivation of adsorbent materials [10,118]. For instance, sulfation/desulfation studies showed that Ag/Al<sub>2</sub>O<sub>3</sub> is very susceptible to sulfur poisoning, resulting in a decrease in its NO<sub>x</sub> storage efficiency from 56 to 36% when 20 ppm of SO<sub>2</sub> was introduced into the feed gas [95]. It was also difficult to regenerate the poisoned catalyst, as only 27% of the adsorbed sulfur was removed from a 1.3 wt% Ag/Al<sub>2</sub>O<sub>3</sub> catalyst after three consecutive desulfations under lean, stoichiometric, and rich conditions up to 630 °C [95]. Sulfur oxide species are acidic and therefore are adsorbed on basic supports [119]. Therefore, increasing the acidity of the material is a promising way for improving its sulfur tolerance and the ease of desulfation. For example, Tsukamoto et al. suggested that doping Ag/Al<sub>2</sub>O<sub>3</sub> catalysts with titania (TiO<sub>2</sub>) increased the acidity of the catalyst and consequently improved its desulfation performance [120].

Zeolite based catalysts tend to be more sulfur resistant compared to oxide based catalysts [112]. Chen et al. showed that exposure to 21 mol of SO<sub>2</sub> per mole of Pd at 100 °C essentially eliminated the NO<sub>x</sub> storage capability of Pd/CeO<sub>2</sub>, but Pd/BEA, Pd/MFI, and Pd/CHA retained most of their NO<sub>x</sub> storage capacities (Fig. 14) [75]. It was suggested that the highly dispersed Pd<sup>2+</sup> at the exchange sites of the zeolite can store NO at low temperatures without being significantly affected by the SO<sub>2</sub>.

These results suggest that sulfur poisoning can cause a major deactivation on the performance of oxide based PNAs. Our knowledge on the effect of sulfur on the performance of zeolite based PNAs is currently limited to a single study [75]. Thus, more attention is required to elucidate the sulfur tolerance of zeolite based PNAs.

### 3.4. Regenerability of PNAs

Similar with the HCTs, PNAs undergo multiple cycles during the life of vehicles and their ability to release NO<sub>x</sub> before the next cycle is a crucial factor for their practical application. Herein, the regenerability of PNAs will be discussed in terms of their NO<sub>x</sub> desorption ability and their reactivation.

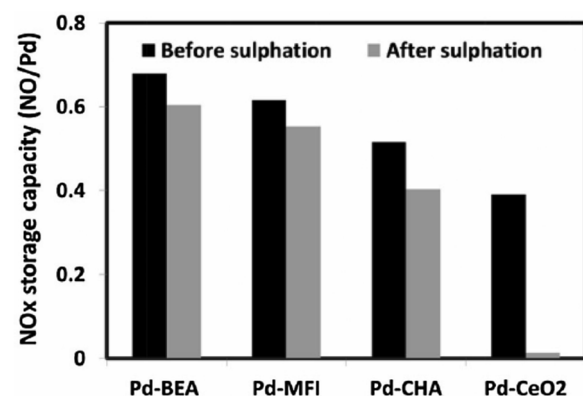


Fig. 14. NO<sub>x</sub> storage capacity at 100 °C over 1 wt.% Pd containing samples before and after sulfation. Zeolites materials have higher sulfur-tolerance compared to oxide materials. Reprinted from Chen et al. [75], Copyright© (2016), with permission from Springer.

#### 3.4.1. Purging of stored NO<sub>x</sub>

After the PNA has adsorbed NO<sub>x</sub> during the cold start period, the majority of the adsorbed NO<sub>x</sub> needs to be desorbed after the vehicle has warmed up to provide available adsorption sites for the next cold start. This desorption of the stored NO<sub>x</sub> needs to occur under normal driving conditions without the need for a special high temperature treatment to purge the PNA. The maximum exhaust temperatures on diesel engines during normal driving typically fall between 250 and 350 °C. Therefore, the PNA needs to be essentially purged of all the stored NO<sub>x</sub> (ideally) by 250 °C or (in the worst case) by 350 °C. However, if the PNA adsorbs much of the NO<sub>x</sub> as nitrates, some of these storage sites may not be purged during normal driving. For instance, doping Pt/γ-Al<sub>2</sub>O<sub>3</sub> with 1 wt% La resulted in the formation of strong NO<sub>x</sub> adsorption sites and led to significant improvement in their initial NO<sub>x</sub> storage efficiency [108]. However, these strong adsorption sites (nitrates) were not fully regenerated during warmed up operation, leading to a continuous decrease in NSE during 5 consecutive cycles. This demonstrated that Pt/Al<sub>2</sub>O<sub>3</sub> and Pt/CZO retained more NO<sub>x</sub> species compared to Pd/Al<sub>2</sub>O<sub>3</sub> and Pd/CZO after desorption [106]. Specifically, 0.45 and 0.25 g/L of NO<sub>x</sub> was retained by Pt/Al<sub>2</sub>O<sub>3</sub> and Pt/CZO, respectively, attributed to nitrate formation. However, only a small amount of NO<sub>x</sub> was retained by Pd/Al<sub>2</sub>O<sub>3</sub> and Pd/CZO after desorption. This indicated that Pd/Al<sub>2</sub>O<sub>3</sub> and Pd/CZO catalysts are more suitable PNA materials in terms of regenerability. Regarding the desorption of NO<sub>x</sub> from zeolite-based PNAs, Chen et al. demonstrated that essentially all of the adsorbed NO<sub>x</sub> was removed from Pd-containing BEA, MFI, and CHA zeolites after ramping the temperature to 400 °C [75].

#### 3.4.2. Reactivation of PNAs

A second mechanism that results in gradual deterioration of the NSE for Pd-based PNAs is the gradual reduction of the Pd oxide. Theis et al. showed that the NSE of a Pd-based PNA decreased gradually when evaluated on consecutive transient tests [12]. Lean CH<sub>4</sub> oxidation was used to infer the oxidation state of the Pd and confirmed that the Pd oxide was partially reduced after only two lean transient tests. This was attributed to the Pd oxide reacting with the NO and C<sub>2</sub>H<sub>4</sub> at low temperatures (e.g., 90 °C) to form NO<sub>2</sub> and CO. The NSE was recovered after a hot lean oxidation, which served to re-oxidize the reduced Pd oxide.

### 3.5. Durability of PNAs

A condition for applying PNAs in vehicle exhaust systems is their capability to maintain their trapping performance after exposure to high temperatures in the presence of water. However, structure changes and/or PGM sintering can occur during hydrothermal aging that can

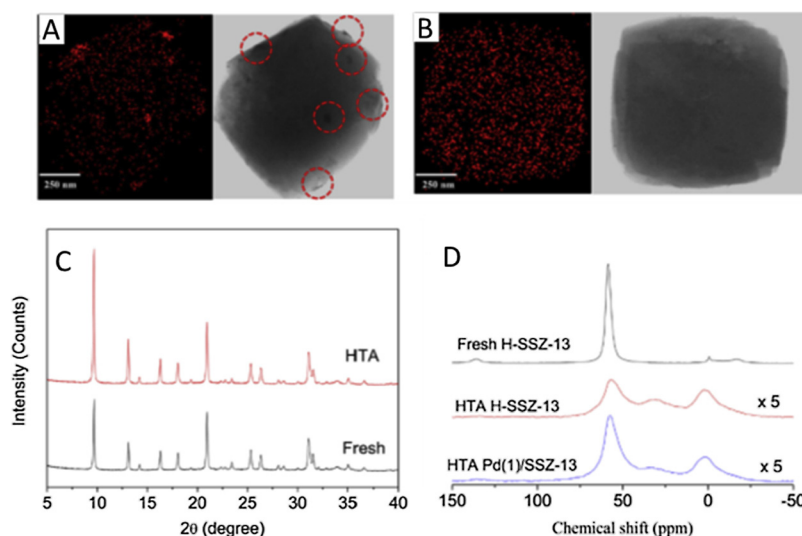


**Fig. 15.** EDS mapping of Pd (left) and Z-contrast STEM images (right) of (A) fresh and (B) hydrothermally aged 1 wt.% Pd/SSZ-13. (C) XRD patterns of fresh and hydrothermally aged 2 wt.% Pd/SSZ-13 catalysts. (D) Solid-state  $^{27}\text{Al}$ -NMR spectra of fresh H-SSZ-13, hydrothermally aged H-SSZ-13 and 1 wt.% Pd/SSZ-13. Upon hydrothermal aging, Pd species are re-distributed in SSZ-13 zeolite. Incorporation of Pd reduces SSZ-13 dealumination. Reprinted from Ryoo et al. [34], Copyright© (2017), with permission from Elsevier.

result in partial deactivation of PNAs. For example, hydrothermal aging ( $750^\circ\text{C}/16\text{ h}$ ) of 1 wt% PdCe20Pr (20 mol% of Pr) led to a significant decrease of the NO<sub>x</sub> storage efficiency, and the desorption temperature decreased from the range of 350–500 °C to below 350 °C [33]. Jones et al. attributed the decrease in the NO<sub>x</sub> storage efficiency and the decrease in desorption temperature to structural changes during aging. Specifically, BET analysis showed a surface area decrease from 66.2 to 18.9 m<sup>2</sup>/g for PdCe20Pr, while the average diameter of the support particles increased in size from 10 to 14.9 nm for Ce20Pr. Moreover, the average Pd particle size in 1 wt% PdCe20Pr increased from 3.99 to 8.3 nm [33]. The three observations corresponded to structural changes of surface area loss, oxide support sintering, and metal sintering. However, it was reported recently that hydrothermal aging at 750 °C for 25 h was able to increase the NO<sub>x</sub> adsorption of Pd containing SSZ-13 zeolites [34]. Interestingly, incorporation of Pd in SSZ-13 zeolite resulted in the prevention of zeolite dealumination (Fig. 15C and D). Furthermore, the initially agglomerated Pd in the fresh sample was homogeneously re-distributed within the zeolite after hydrothermal aging (Fig. 15A and B), thus enhancing the NO<sub>x</sub> adsorption.

The results above demonstrate that PGM sintering and reduction of the support surface area after hydrothermal aging are both major factors that can result in complete or partial deactivation of oxide based PNAs. While similar results were expected for zeolite based PNAs, a promising recent study showed that Pd re-distribution can occur after hydrothermal aging when durable SSZ-13 zeolite was used as a support. In this isolated case, hydrothermal aging resulted in enhancement of NO<sub>x</sub> adsorption. Development of zeolites with improved hydrothermal stability will be of a key interest for future PNA applications.

#### 4. Conclusions and outlook

The current state-of-the-art for HC and NO<sub>x</sub> trapping technologies is promising. However, underlying performance descriptors are only emerging or remain unknown. The trapping technology performance depends upon the trapping material, the feedstream composition, and exhaust conditions such as space velocity and temperature. Zeolites have become the HC trapping materials of choice due to their ability to trap hydrocarbons at low temperatures and convert them to other species at higher temperatures as the vehicle warms up. The acidity properties of zeolites influence the HC adsorption efficiency because each acid site (Brønsted or Lewis) interacts differently with HCs. The HC trapping capability of zeolite materials can be improved through ion-exchanging with metal cations, likely by improving the number of adsorption sites [40]. The pore sizes of zeolites can affect their HC adsorption capacity by restricting or even preventing bulky molecules

(e.g. toluene) from diffusing through them [75]. During desorption, the trapped HCs can undergo oxidation reactions when oxygen is present or partial oxidation reactions when oxygen is limited or absent [41,72]. However, small molecules such as alkenes can undergo oligomerization reactions under certain conditions, which result in molecules that can block the zeolite pores [57].

Early research into passive NO<sub>x</sub> adsorbers focused on metal oxides (e.g., CeO<sub>2</sub>, Al<sub>2</sub>O<sub>3</sub>) modified with precious metals (e.g., Pt, Pd). The NO<sub>x</sub> storage efficiency of oxide based traps can be improved with the addition of dopants (e.g., Pr and La). A major concern for Pt based oxide catalysts is the formation of nitrates because it is difficult to fully regenerate the nitrates and free up the storage sites for the next cold start. Thus, Pd based PNAs are preferred because they store much of the NO<sub>x</sub> as nitrites, which can be decomposed more easily during normal driving conditions. However, low NO<sub>x</sub> storage efficiencies, inhibition from H<sub>2</sub>O at temperature below 100 °C, and sulfur poisoning remain as significant issues for the oxide based catalysts.

Research is just now emerging on the investigation of zeolites for passive NO<sub>x</sub> adsorption. Unexchanged zeolites are not effective for storing NO<sub>x</sub>. However, significantly more NO<sub>x</sub> can be adsorbed on Pd ion-exchanged zeolites, attributed to the formation of nitrosyls on the Pd sites [75]. Small pore zeolites have a higher binding energy of NO<sub>x</sub> compared to larger pore zeolites, resulting in higher desorption temperatures. Significant advantages of zeolite-based PNAs over metal oxide PNAs are their improved tolerance to H<sub>2</sub>O at low temperatures and their improved sulfur tolerance.

In addition to high storage efficiency, the HCTs and PNAs must be durable under high temperature conditions. Collapsing of the zeolite crystalline structure upon thermal aging can lead to a decrease of the HC adsorption and NO<sub>x</sub> adsorption capacities [80,106]. During thermal aging in zeolites, the process of dealumination occurs, where zeolite framework aluminum leaves and forms deposited extra-framework aluminum. Some HCs can increase their storage efficiency by interacting with this extra-framework aluminum. But overall, hydrothermal aging exhibits detrimental effects on the HC storage efficiency of zeolites. To date, little has been reported on the effect of high temperature aging on zeolite based PNAs. Under certain conditions, re-distribution of the PdO in Pd/SSZ-13 zeolite after aging resulted in an enhancement of its NO<sub>x</sub> adsorption capacity [34].

#### Acknowledgements

The authors are grateful to Eric Walker of the University of Michigan for his helpful advice and his review of the manuscript. The authors would also like to acknowledge Jason Lupescu of Ford Motor

Company for helpful discussions. The authors are supported by start-up funding from the UB Department of Chemical and Biological Engineering.

## References

- [1] A.P. Wong, E.A. Kyriakidou, T.J. Toops, J.R. Regalbuto, The catalytic behavior of precisely synthesized Pt-Pd bimetallic catalysts for use as diesel oxidation catalysts, *Catal. Today* 267 (2016) 145–156.
- [2] S. Du, W. Tang, Y. Guo, A. Binder, E.A. Kyriakidou, T.J. Toops, S. Wang, Z. Ren, S. Hoang, P.-X. Gao, Understanding low temperature oxidation activity of nano-array based monolithic catalysts: from performance observation to structural and chemical insights, *Emiss. Control Sci. Technol.* 3 (2017) 18–36.
- [3] M.-Y. Kim, E.A. Kyriakidou, J.-S. Cho, T.J. Toops, A.J. Binder, C. Thomas, J.E. Parks II, V. Schwartz, J. Chen, D.K. Hensley, Enhancing low-temperature activity and durability of Pd-based diesel oxidation catalysts using  $ZrO_2$  supports, *Appl. Catal. B* 187 (2016) 181–194.
- [4] U.S. Environmental Protection Agency, EPA Proposes Tier 3 Motor Vehicle Emission and Fuel Standards, U.S. Environmental Protection Agency, EPA-420-F-13-016a, (2013), pp. 1–4.
- [5] A. Westermann, B. Azambre, Impact of the zeolite structure and acidity on the adsorption of unburnt hydrocarbons relevant to cold start conditions, *J. Phys. Chem. C* 120 (45) (2016) 25903–25914.
- [6] Y. Zheng, L. Kovarik, M.H. Engelhard, Y. Wang, Y. Wang, F. Gao, J. Szanyi, Low-temperature Pd/zeolite passive NOx Adsorbers: structure, performance, and adsorption chemistry, *J. Phys. Chem. C* 121 (29) (2017) 15793–15803.
- [7] V.L. Temerev, A.A. Vedyagin, T.N. Afonasenko, K.N. Iost, Y.S. Kotolevich, V.P. Baltakhinov, P.G. Tyurulinov, Effect of Ag loading on the adsorption/desorption properties of ZSM-5 towards toluene, *React. Kinet. Mech. Catal.* 119 (2) (2016) 629–640.
- [8] M. Sharma, M. Shafe, Hydrocarbon-water adsorption and simulation of catalyzed hydrocarbon traps, *Catal. Today* 267 (2016) 82–92.
- [9] E.A. Kyriakidou, T.J. Toops, J.-S. Choi, M.J. Lance, J.E. Parks II, Exhaust treatment catalysts with enhanced hydrothermal stability and low-temperature activity, US Patents US20180250659A1 (2018).
- [10] H.-Y. Chen, S. Mulla, E. Weigert, K. Camm, T. Ballinger, J. Cox, P. Blakeman, Cold start concept (CSC™): a novel catalyst for cold start emission control, *SAE Int. J. Fuels Lubr.* 6 (2) (2013) 372–381.
- [11] J. Theis, C. Lambert, The effects of CO,  $C_2H_4$ , and  $H_2O$  on the NOx storage performance of low temperature NOx adsorbers for diesel applications, *SAE Int. J. Engines* 10 (4) (2017) 1627–1637.
- [12] S. Jones, Y. Ji, M. Crocker, Ceria-based catalysts for low temperature NOx storage and release, *Catal. Lett.* 146 (2016) 909–917.
- [13] J. Theis, C.K. Lambert, An assessment of low temperature NOx adsorbers for cold start NOx control on diesel engines, *Catal. Today* 258 (2015) 367–377.
- [14] M.J. Hazlett, W.S. Epling, Spatially resolving CO and  $C_2H_6$  oxidation reactions in a Pt/ $Al_2O_3$  model oxidation catalyst, *Catal. Today* 267 (2016) 157–166.
- [15] C. Kim, M. Schmid, S.J. Schmiege, J. Tan, W. Li, The Effect of Pt-Pd Ratio on Oxidation Catalysts Under Simulated Diesel Exhaust, *SAE Tech. Pap.* 2011-01-1134, (2011).
- [16] J.E. Etheridge, T.C. Watling, A.J. Izzard, M.A.J. Paterson, The effect of Pt:Pd ratio on light duty diesel oxidation catalyst performance: an experimental and modeling study, *SAE Int. J. Engines* 8 (3) (2015) 1283–1299.
- [17] B.M. Shakya, B. Sukumar, Y.M. López-De-Jesús, P. Markatou, The effect of Pt:Pd ratio on heavy-duty diesel oxidation catalyst performance: an experimental and modeling study, *SAE Int. J. Engines* 8 (3) (2015) 1271–1282.
- [18] Y. Kobatake, K. Momma, S.P. Elangovan, K. Itabashi, T. Okubo, M. Ogura, “Super hydrocarbon reformer trap” for the complete oxidation of toluene using iron-exchanged  $\beta$ -Zeolite with a low Silicon/Aluminum ratio, *ChemCatChem* 8 (2016) 2516–2524.
- [19] C.-L. Myung, J. Kim, W. Jang, D. Jin, S. Park, J. Lee, Nanoparticle filtration characteristics of advanced metal foam media for a spark ignition direct injection engine in steady engine operation conditions and vehicle test modes, *Energies* 8 (2015) 1865–1881.
- [20] J.-H. Park, S.J. Park, I.-S. Nam, G.K. Yeo, J.K. Kil, Y.K. Youn, A fast quantitative assay for developing zeolite-type hydrocarbon trap catalyst, *Microporous Mesoporous Mater.* 101 (2007) 264–270.
- [21] Z. Sarshar, M.H. Zahedi-Niaki, Q. Huang, M. Eić, S. Kaliaguine, MTW zeolites for reducing cold-start emissions of automotive exhaust, *Appl. Catal. B* 87 (2009) 37–45.
- [22] B. Pérez-Ortíz, L. García-Andújar, T. García, M.V. Navarro, S. Mitchell, J. Pérez-Ramírez, Bifunctional Cu/H-ZSM-5 zeolite with hierarchical porosity for hydrocarbon abatement under cold-start conditions, *Appl. Catal. B* 154–155 (2014) 161–170.
- [23] A. Westermann, B. Azambre, G. Finqueneisel, P. Da Costa, F. Can, Evolution of unburnt hydrocarbons under “cold-start” conditions from adsorption/desorption to conversion: on the screening of zeolitic materials, *Appl. Catal. B* 158–159 (2014) 48–59.
- [24] F. Migliardini, F. Iuolano, D. Caputo, P. Corbo, MFI and FAU-Type zeolites as trapping materials for light hydrocarbons emission control at low partial pressure and high temperature, *J. Chem. (Hindawi Online)* 2015 (2015).
- [25] K.F. Czaplewski, T.L. Reitz, Y.J. Kim, R.Q. Snurr, One-dimensional zeolites as hydrocarbon traps, *Microporous Mesoporous Mater.* 56 (2002) 55–64.
- [26] T. Minami, T. Nagase, Exhaust gas purification device in variable combination of absorbent and catalyst according to gas temperature, US Patent US005140811A (1992).
- [27] Y. Myrate, T. Morita, K. Wada, H. Ohno, NOx trap three-way catalyst (N-TWC) concept: TWC with NOx adsorption properties at low temperatures for cold-start emission control, *SAE Int. J. Fuels Lubr.* 8 (2) (2015) 454–459.
- [28] J.K. Hochmuth, P.L. Burk, C. Tolentino, M.J. Mignano, Hydrocarbon traps for controlling cold start emissions, *SAE Tech. Pap.* (1993) 930739.
- [29] R.G. Silver, D. Dou, C.W. Kirby, R.P. Richmond, J. Balland, A durable in-line hydrocarbon adsorber for reduced cold start exhaust emissions, *SAE Tech. Pap.* (1997) 972843.
- [30] Y. Hiramoto, M. Takaya, S. Yamamoto, A. Okada, Development of a new HC-Adsorption three-way catalyst system for Partial-ZEV performance, *SAE Tech. Pap.* (2003) 2003-01-1861.
- [31] J.E. Coulson, R.J. Brisley, O. Keane, P.R. Phillips, E.H. Mountstevens, Thermally regenerable nitric oxide adsorbent, Patent Application, WO 2008047170A1 (2008).
- [32] J. Nunan, J. Lupescu, G. Denison, D. Ball, D. Moser, HC traps for gasoline and ethanol applications, *SAE Int. J. Fuels Lubr.* 6 (2) (2013) 430–449.
- [33] S. Jones, Y. Ji, A. Bueno-Lopez, Y. Song, M. Crocker,  $CeO_2\text{-}M_2O_3$  passive NOx adsorbers for cold start applications, *Emiss. Control Sci. Technol.* 3 (2017) 59–72.
- [34] Y.S. Ryou, J. Lee, S.J. Cho, H. Lee, C.H. Kim, D.H. Kim, Activation of Pd/SSZ-13 catalyst by hydrothermal aging treatment in passive NO adsorption performance at low temperature for cold start application, *Appl. Catal. B* 212 (2017) 140–149.
- [35] G. Cavataio, J.A. Lupescu, S. Elwart, J.M. Kerns, M.J. Uhrich, Hydrocarbon and NOx trap, US Patent US20110061371A1 (2011).
- [36] P.J. Wesson, R.Q. Snurr, Modified temperature programmed desorption evaluation of hydrocarbon trapping by CsMOR zeolite under cold start conditions, *Microporous Mesoporous Mater.* 125 (2009) 35–38.
- [37] R. Yoshimoto, K. Hara, K. Okumura, N. Katada, M. Niwa, Analysis of toluene adsorption on Na-Form zeolite with a temperature-programmed desorption method, *J. Phys. Chem. C* 111 (3) (2007) 1474–1479.
- [38] T. Kanazawa, Development of hydrocarbon adsorbents, oxygen storage materials for three-way catalysts and NOx storage-reduction catalyst, *Catal. Today* 96 (2004) 171–177.
- [39] B.A. De Moor, M.-F. Reyniers, O.C. Gobin, J.A. Lercher, G.B. Marin, Adsorption of  $C_2\text{-}C_8$  n-Alkanes in zeolites, *J. Phys. Chem. C* 115 (4) (2011) 1204–1219.
- [40] S.P. Elangovan, M. Ogura, M.E. Davis, T. Okubo, SSZ-33: a promising material for use as a hydrocarbon trap, *J. Phys. Chem. B* 108 (35) (2004) 13059–13061.
- [41] A. Westermann, B. Azambre, M. Chebbi, A. Koch, Modification of Y Faujasite zeolites for the trapping and elimination of a propene-toluene-decane mixture in the context of cold-start, *Microporous Mesoporous Mater.* 230 (2016) 76–88.
- [42] S.B. Kang, C. Kalamaras, V. Balakotaiah, W. Epling, Hydrocarbon trapping over Ag-Beta zeolite for cold-start emission control, *Catal. Lett.* 147 (6) (2017) 1355–1362.
- [43] R.J. Brisley, N.R. Collins, D. Law, Catalytic purification of engine exhaust gas, European Patent Application EP0716877A1 (1996).
- [44] J.S. Hepburn, H.-W. Jen, H.S. Gandhi, K. Otto, Catalyst/hydrocarbon trap hybrid system, US Patent US005772972A (1998).
- [45] J.A. Lupescu, H. Jen, Combined hydrocarbon trap and catalyst, US Patent US20130287659A1 (2013).
- [46] C.T. Goralski, T. Chanko, J. Lupescu, G. Ganti, Experimental and modeling investigation of catalyzed hydrocarbon trap performance, *SAE Tech. Pap.* (2000) 2000-01-0654.
- [47] S. Yamamoto, K. Matsushita, S. Etoh, M. Takaya, In-line hydrocarbon (HC) adsorber system for reducing cold-start emission, *SAE Tech. Pap.* (2000) 2000-01-0892.
- [48] C. Goralski, J. Lupescu, T. Chanko, J. Hepburn, Application of catalyzed hydrocarbon traps to reduce hydrocarbon emission from ethanol flex-fuel vehicles, *SAE Tech. Pap.* (1999) 1999-01-3624.
- [49] T.H. Ballinger, P.J. Andersen, Vehicle comparison of advanced three-way catalyst and hydrocarbon trap catalysts, *SAE Tech. Pap.* (2002) 2002-01-0730.
- [50] J.A. Lupescu, H. Jen, J.S. Hepburn, Hydrocarbon trap having improved adsorption capacity, US Patent US20140044625A1 (2014).
- [51] G. Cavataio, J.A. Lupescu, M. Sharma, Hydrocarbon trap with increased zeolite loading and improved adsorption capacity, US Patent US20150209769A1 (2015).
- [52] L. Xu, R.W. McCabe, J.A. Lupescu, Low temperature catalyst/hydrocarbon trap, US Patent US20150231566A1 (2015).
- [53] P.G. Blakeman, E.M. Burkholder, H.-Y. Chen, J.E. Collier, J.M. Fedeyko, H. Jobson, R.R. Rajaram, The role of pore size on the thermal stability of zeolites supported Cu SCR catalyst, *Catal. Today* 231 (2014) 56–63.
- [54] J.-Y. Luo, H. Oh, C. Henry, W. Epling, Effect of  $C_3H_6$  on selective catalytic reduction of NOx over a Cu/zeolite catalyst: a mechanistic study, *Appl. Catal. B* 123–124 (2012) 296–305.
- [55] S.P. Elangovan, M. Ogusa, S. Ernst, M. Hartmann, S. Tontisirin, M.E. Davis, T. Okubo, A comparative study of zeolites SSZ-33 and MCM-68 for hydrocarbon trap applications, *Microporous Mesoporous Mater.* 96 (2006) 210–215.
- [56] J.-H. Park, S.J. Park, H.A. Ahn, I.-S. Nam, G.K. Yeo, J.K. Kil, Y.K. Youn, Promising zeolite-type hydrocarbon trap catalyst by a knowledge-based combinatorial approach, *Microporous Mesoporous Mater.* 117 (2009) 178–184.
- [57] F. Geobaldo, G. Spoto, S. Bordiga, C. Lamberti, A. Zecchina, Propene oligomerization on H-mordenite: hydrogen-bonding interaction, chain initiation, propagation and hydrogen transfer studied by temperature-programmed FTIR and UV-VIS spectroscopies, *J. Chem. Soc. Faraday Trans.* 93 (1997) 1243–1249.
- [58] A.A. Adamczyk, A.D. Logan, Polymerization catalyst enhanced hydrocarbon trapping process, US Patent US5814287A (1998).
- [59] Y. Li, Y. Wang, X. Liu, X. Li, R. Pan, P. Han, T. Dou, Synthesis of hierarchical mesoporous zeolites based on MOR zeolite: application in the automobile tailpipe

hydrocarbon trap, *J. Porous Mater.* 22 (2015) 807–815.

[60] B. Azambre, A. Westermann, G. Finqueneisel, F. Can, J.D. Comparot, Adsorption and desorption of a model hydrocarbon mixture over HY zeolite under dry and wet conditions, *J. Phys. Chem. C* 119 (2015) 315–331.

[61] E. Yoda, J.N. Kondo, K. Domen, Detailed process of adsorption of alkanes and alkenes on zeolites, *J. Phys. Chem. B* 109 (4) (2005) 1464–1472.

[62] I. Daldoul, S. Auger, P. Picard, B. Nohair, S. Kaliaguine, Effect of temperature Ramp on hydrocarbon desorption profiles from ZSM-12, *Can. J. Chem. Eng.* 94 (2016) 931–937.

[63] R.W. Dorner, M. Deifallah, C.R.A. Catlow, F. Corá, S.P. Elangovan, T. Okubo, G. Sankar, Heteroatom-substituted microporous AFI and ATS structured materials for hydrocarbon trap: an insight into the aluminophosphate framework-toluene interaction, *J. Phys. Chem. C* 112 (11) (2008) 4187–4194.

[64] Y. Takamitsu, K. Ariga, S. Yoshida, G. Ogawa, T. Sano, Adsorption of toluene on alkali metal ion-exchanged ZSM-5 and  $\beta$ -Zeolites under humid conditions, *Bull. Chem. Soc. Jpn.* 85 (8) (2012) 869–876.

[65] R.M. Serra, E.E. Miró, P. Bolcato, A.V. Boix, Experimental and theoretical studies about the adsorption of toluene on ZSM5 and mordenite zeolites modified with Cs, *Microporous Mesoporous Mater.* 147 (2012) 17–29.

[66] J.A. Lupescu, H. Jen, Hydrocarbon trap for reducing cold-start engine emission, US Patent US8926910B2 (2015).

[67] I. Perdama, D. Creaser, T. Öhrman, J. Hedlund, A comparison of NO<sub>x</sub> adsorption on Na, H and Ba/ZSM-5 films, *Appl. Catal. B* 72 (1-2) (2007) 82–91.

[68] W. Hertl, I. M. Lachman, Modified large pore zeolites for trapping alkenes, European Patent Application EP0639400A1 (1995).

[69] V.R. Choudhary, K.R. Srinivasan, A.P. Singh, Temperature-programmed desorption of aromatic hydrocarbons on silicalite-I and ZSM-5-type zeolites, *Zeolites* 10 (1) (1990) 16–20.

[70] J.K. Lampert, M. Deeba, R.J. Farrauto, Catalyzed hydrocarbon trap material and method of making the same, US patent US006074973A (2000).

[71] X. Liu, J.K. Lampert, D.A. Arendarskiia, R.J. Farrauto, FT-IR spectroscopic studies of hydrocarbon trapping in Ag<sup>+</sup>-ZSM-5 for gasoline engines under cold-start conditions, *Appl. Catal. B* 35 (2) (2001) 125–136.

[72] M. Navlani-Garcia, B. Puertolas, D. Lozano-Castello, D. Cazorla-Amoros, M.V. Navarro, T. García, CuH-ZSM-5 as hydrocarbon trap under cold start conditions, *Environ. Sci. Technol.* 47 (11) (2013) 5851–5855857.

[73] M.D. Patil, I.M. Lachman, Modified zeolite for trapping hydrocarbons, European Patent Application EP0640381A1 (1995).

[74] B. Puertolas, M. Navlani-García, T. García, M.V. Navarro, D. Lozano-Castelló, D. Cazorla-Amorós, Optimizing the performance of catalytic traps for hydrocarbon abatement during the cold-start of a gasoline engine, *J. Hazard. Mater.* 279 (2014).

[75] H.-Y. Chen, J.E. Collier, D. Liu, L. Mantarosie, D. Durán-Martín, V. Novák, R.R. Rajaram, D. Thompson, Low Temperature NO Storage of zeolite supported Pd for low temperature diesel engine emission control, *Catal. Lett.* 146 (9) (2016) 1706–1711.

[76] R.M. Serra, E.E. Miró, M.K. Sapag, A.V. Boix, Adsorption and diffusion of toluene on Na and Cs mordenites for hydrocarbon traps, *Microporous Mesoporous Mater.* 138 (2011) 102–109.

[77] G.S. Bugosh, M.P. Harold, Impact of zeolite Beta on hydrocarbon trapping and light-off behavior on Pt/Pd/BEA/Al<sub>2</sub>O<sub>3</sub> monolith catalysts, *Emiss. Control Sci. Technol.* 3 (2017) 123–134.

[78] A.A. Adamczyk, C.T. Goralski, W.P. Boone, Method and apparatus to improve catalyzed hydrocarbon trap efficiency, US Patent US0094035A1 (2004).

[79] A. Ilyas, H.M. Zahedi-Niaki, M. Eić, One-dimensional molecular sieves for hydrocarbon cold-start emission control: influence of water and CO<sub>2</sub>, *Appl. Catal. A Gen.* 382 (2010) 213–219.

[80] J. Luo, R.W. McCabe, M.A. Dearth, R.J. Gorte, Transient adsorption studies of automotive hydrocarbon traps, *AIChE J.* 60 (8) (2014) 2875–2881.

[81] A. Ignaczak, J.A.N.F. Gomes, A theoretical study of the interaction of water molecules with the Cu(100), Ag(100) and Ag(100) surfaces, *J. Electroanal. Chem.* 420 (1997) 209–218.

[82] T.H. Yeon, H.S. Han, E.D. Park, J.E. Yie, Adsorption and desorption characteristics of hydrocarbons in multi-layered hydrocarbon traps, *Microporous Mesoporous Mater.* 119 (2009) 349–355.

[83] D.S. Lafayatis, G.P. Ansell, S.C. Bennett, J.C. Frost, P.J. Millington, R.R. Rajaram, A.P. Walker, T.H. Ballinger, Ambient temperature light-off for automobile emission control, *Appl. Catal. B* 18 (1998) 123–135.

[84] T.H. Ballinger, P.J. Andersen, Hydrocarbon trap/catalyst for reducing cold-start emissions from internal combustion engines, US Patent US6617276B1 (2003).

[85] A.G. Stepanov, M.V. Luzgin, V.N. Romanikov, V.N. Sidelnikov, E.A. Paukshtis, The Nature, Structure, and Composition of Adsorbed Hydrocarbon Products of Ambient Temperature Oligomerization of Ethylene on Acidic Zeolite H-ZSM-5, *J. Catal.* 178 (1998) 466–477.

[86] N.R. Burke, D.L. Trimm, R.F. Howe, The effect of silica:alumina ratio and hydrothermal ageing on the adsorption characteristics of BEA zeolites for cold start emission control, *Appl. Catal. B* 46 (2003) 97–104.

[87] S.G. Aspromonte, R.M. Serre, E.E. Miró, A.V. Boix, AgNaMordenite catalysts for hydrocarbon adsorption and deNO<sub>x</sub> processes, *Appl. Catal. A Gen.* 407 (2011) 134–144.

[88] B. Puertolas, J.M. López, M.V. Navarro, T. García, R. Murillo, A.M. Mastral, F.J. Varela-Gandía, D. Lozano-Castelló, A. Bueno-López, D. Cazorla-Amorós, Abatement of hydrocarbons by acid BETA and ZSM-5 zeolites under cold-start conditions, *Adsorption* 19 (2013) 357–365.

[89] F. Geobaldo, G. Spoto, S. Bordiga, C. Lamberti, A. Zecchina, Propene oligomerization on H-mordenite: hydrogen-bonding interaction, chain initiation, propagation and hydrogen transfer studied by temperature-programmed FTIR and UV-VIS spectroscopies, *J. Chem. Soc. Faraday Trans.* 93 (1997) 1243–1249.

[90] J.R. Trudell, Contributions of dipole moments, quadrupole moments, and molecular polarizabilities to the anesthetic potency of fluorobenzenes, *Biophys. Chem.* 73 (1998) 7–11.

[91] J.A. Lupescu, T.B. Chanko, J.F. Richert, A.A. Mauti, The effect of spark timing on engine-out hydrocarbon speciation and hydrocarbon trap performance, *SAE Tech. Pap.* (2009) 2009-01-1068.

[92] J.P. Van den Berg, J.P. Wolthuizen, A.D.H. Clague, G.R. Hays, R. Huis, J.H.C. van Hooff, Low-temperature oligomerization of small olefins on zeolite H-ZSM-5: An investigation with high-resolution solid-state C<sup>13</sup>-NMR, *J. Catal.* 80 (1983) 130–138.

[93] P. Yarlagadda, C.R.F. Lund, E. Ruckenstein, Oligomerization of ethene and propene over composite zeolite catalysts, *Appl. Catal.* 62 (1) (1990) 125–139.

[94] M. Navlani-Garcia, F.J. Varela-Gandía, A. Bueno-López, D. Cazorla-Amorós, B. Puertolas, J.M. Lopez, T. García, D. Lozano-Castello, BETA zeolite thin films supported on honeycomb monoliths with tunable properties as hydrocarbon traps under cold-start conditions, *ChemSusChem* 6 (2013) 1467–1477.

[95] S. Ren, S.J. Schmieg, C.K. Koch, G. Qi, W. Li, Investigation of Ag-based low temperature NO<sub>x</sub> adsorbers, *Catal. Today* 258 (2015) 378–385.

[96] F. Millo, D. Vezza, Characterization of a new advanced diesel oxidation catalyst with low temperature NO<sub>x</sub> storage capability for LD diesel, *SAE Tech. Pap.* (2012) 2012-01-0373.

[97] K.C.C. Kharas, O.H. Bailey, J. Vuichard, Improvements in intimately coupled diesel hydrocarbon Adsorber/Lean NO<sub>x</sub> catalysis leading to durable euro 3 performance, *SAE Tech. Pap.* (1998) 982603.

[98] H. Yamazaki, T. Endo, M. Ueno, S. Sugaya, Research on HC adsorption emission system, *SAE Tech. Pap.* (2004) 2004-01-1273.

[99] Ch. Minchev, V. Minkov, V. Penchev, H. Weyda, H. Lechner, Thermal-decomposition of tripropylamine as a template in MEAPO-5 molecular-sieves, *J. Therm. Anal.* 37 (1991) 171–181.

[100] B. Moden, J.M. Donohue, W.E. Cormier, H.-X. Li, The uses and challenges of zeolites in automotive applications, *Top. Catal.* 53 (2010) 1367–1373.

[101] L. Ding, Y. Zheng, Y. Hong, Z. Ring, Effect of particle size on the hydrothermal stability of zeolite beta, *Microporous Mesoporous Mater.* 101 (2007) 432–439.

[102] A. Ilyas, M.H. Zahedi-Niaki, M. Eić, S. Kaliaguine, Control of hydrocarbon cold-start emissions: A search for potential adsorbents, *Microporous Mesoporous Mater.* 102 (2007) 171–177.

[103] M.E. Davis, T. Okubo, Molecular sieves for improved hydrocarbon traps, US Patent US20050166581 (2005).

[104] S.P. Elangovan, M. Ogura, Y. Zhang, N. Chino, T. Okubo, Silicoaluminophosphate molecular sieves as a hydrocarbon trap, *Appl. Catal. B* 57 (2005) 31–36.

[105] M. Briand, A. Shikholeslami, M.-J. Peltre, D. Delafosse, D. Barthomeuf, Thermal and hydrothermal stability of SAPO-5 and SAPO-37 molecular-sieves, *J. Chem. Soc., Dalton Trans.* 7 (1989) 1361–1362.

[106] N. Noda, A. Takahashi, Y. Shibagaki, H. Mizuno, In-line hydrocarbon adsorber for cold start emissions – part II, *SAE Tech. Pap.* (1998) 980423.

[107] J. Theis, An assessment of Pt and Pd model catalysts for low temperature NO<sub>x</sub> adsorption, *Catal. Today* 267 (2016) 93–109.

[108] Y. Ji, S. Bai, M. Crocker, Al<sub>2</sub>O<sub>3</sub>-based passive NO<sub>x</sub> adsorbers for low temperature applications, *Appl. Catal. B* 170–171 (2015) 283–292.

[109] X. Chang, G. Lu, Y. Guo, Y. Wang, Y. Guo, A high effective adsorbent of NO<sub>x</sub>: preparation, characterization and performance of Ca-beta zeolites, *Microporous Mesoporous Mater.* 165 (2013) 113–120.

[110] J.E. Collier, Passive NO<sub>x</sub> adsorber, US Patent US20160279598A1 (2016).

[111] J.E. Collier, S. Yang, Passive NO<sub>x</sub> adsorber, US Patent US20130001169A1 (2017).

[112] R.R. Rajaram, H.-Y. Chen, D. Liu, Passive NO<sub>x</sub> adsorber, US Patent US10005075B2 (2018).

[113] W.B. Li, X.F. Yang, L.F. Chen, J.A. Wang, Adsorption/desorption of NO<sub>x</sub> on MnO<sub>2</sub>/ZrO<sub>2</sub> oxides prepared in reverse microemulsions, *Catal. Today* 148 (2009) 75–80.

[114] K. Khivantsev, F. Gao, L. Kovarik, Y. Wang, J. Szanyi, Molecular level understanding of how oxygen and carbon monoxide improve NO<sub>x</sub> storage in palladium/SSZ-13 passive NO<sub>x</sub> adsorber (PNA): The Role of NO<sup>+</sup> and Pd(II)(CO)(NO) Species, *J. Phys. Chem. C* 122 (2018) 10820–10827.

[115] T. Kobayashi, T. Yamada, K. Kayano, Study of NO<sub>x</sub> trap reaction by thermodynamic calculation, *SAE Tech. Pap.* (1997) 970745.

[116] J. Pihl, Washington, DC“Joint Development and Coordination of Emission Control Data and Models (CLEERS Analysis and Coordination”, Oral Presentation at 2018 Annual Merit Review 2018, “Joint Development and Coordination of Emission Control Data and Models (CLEERS Analysis and Coordination”, Oral Presentation at 2018 Annual Merit Review (2018).

[117] A. Vu, J. Luo, J. Li, W.S. Epling, Effects of CO on Pd/BEA passive NO<sub>x</sub> adsorbers, *Catal. Lett.* 147 (2017) 745–750.

[118] E.C. Corbos, X. Courtois, N. Bion, P. Marecot, D. Duprez, Impact of the support oxide and Ba loading on the sulfur resistance and regeneration of Pt/Ba/support catalysts, *Appl. Catal. B* 80 (2008) 62–71.

[119] S. Matsumoto, Y. Ikeda, H. Suzuki, M. Ogai, N. Miyoshi, NO<sub>x</sub> storage-reduction catalyst for automotive exhaust with improved tolerance against sulfur poisoning, *Appl. Catal. B* 25 (2000) 115–124.

[120] Y. Tsukamoto, H. Nishioka, D. Imai, Y. Sobue, N. Takagi, T. Tanaka, T. Hamaguchi, Development of new concept catalyst for low CO<sub>2</sub> emission diesel engine using NO<sub>x</sub> adsorption at low temperatures, *SAE Tech. Pap.* (2012) 2012-01-0370.